# Chapter 10
# Engineering Aspects of Bioluminescence Resonance Energy Transfer Systems

**Abhijit De, Rohit Arora and Akshi Jasani**

## Abbreviations

| | |
|---|---|
| PPI/PPIs | Protein–protein interaction(s) |
| ELISA | Enzyme-linked Immunosorbent Assay |
| Y2H | Yeast two-hybrid assay |
| IY2H | Induced Yeast two-hybrid assay |
| PCAs | Protein-fragment complementation assays |
| FRET | Fluorescence resonance energy transfer |
| BRET | Bioluminescence resonance energy transfer |
| BL | Bioluminescence |
| RLuc | *Renilla* luciferase |
| FLuc | Firefly luciferase |
| ATP | Adenosine triphosphate |
| $LH_2$ | D-Luciferin substrate for FLuc |
| AMP | Adenosine monophosphate |
| $CO_2$ | Carbon dioxide |
| $Em_{max}$ | Emission maximum |
| Clz | Coelenterazine |
| RET | Resonance energy transfer |
| $E_{RET}$ | Efficiency of resonance energy transfer |
| FP/FPs | Fluorescent protein(s) |
| GFP | Green fluorescent protein |
| EYFP | Enhanced yellow fluorescent protein |
| $Ex_{max}$ | Excitation maximum |
| $C_f$ | Correction factor |
| Clz-*h* | Coelenterazine-*h* |

A. De (✉) · R. Arora · A. Jasani
Molecular Functional Imaging Lab, ACTREC, Tata Memorial Centre, Sector 22, Kharghar, Navi Mumbai, Maharashtra 410210, India
e-mail: ade@actrec.gov.in

R. Arora
e-mail: rohit0288@gmail.com

A. Jasani
e-mail: akshi.aj@gmail.com

W. Cai (ed.), *Engineering in Translational Medicine*,
DOI: 10.1007/978-1-4471-4372-7_10, 

| | |
|---|---|
| RFP | Red fluorescent protein |
| Clz-*v* | Coelenterazine-*v* |
| CBP | Coelenterazine-binding protein |
| RLuc-m | *Renilla muelleri* luciferase |
| BLI | Bioluminescence imaging |
| MLuc | *Metridia* luciferase |
| OLuc | *Oplophorus* luciferase |
| CBG | Click beetle green luciferase |
| GLuc | *Gaussia* luciferase |
| VLuc | *Vargula* luciferase |
| NLuc | NanoLuc$^{TM}$ |
| OLuc-19 | 19-kDa catalytic domain of OLuc |
| OLuc-35 | 35-kDa stabilizing domain of OLuc |
| wtGFP | Wild-type green fluorescent protein |
| avGFP | Green fluorescent protein from *Aequorea victoria* |
| EGFP | Enhanced green fluorescent protein |
| RFP | Red fluorescent protein |
| SRET | Sequential resonance energy transfer |
| BiFC-BRET | Bimolecular fluorescence complementation-bioluminescence resonance energy transfer |
| CODA-RET | Complemented donor–acceptor resonance energy transfer |
| BiLC-BiFC | Bimolecular luminescence complementation-bimolecular fluorescence complementation |
| NST | Nocistatin |
| N/OFQ | Nociceptin/Orphanin FQ |
| HIV | Human immunodeficiency virus |
| PR | Protease |
| HTS | High-throughput screening |
| FCV | Feline calicivirus |
| RG | Arginine–glycine peptide |
| CRET | Chemiluminescence resonance energy transfer |
| tdTA | tdTomato-aequorin system |
| CaM | Calmodulin |
| cpVenus | Circularly permuted Venus |
| cpFPs | Circularly permuted fluorescent proteins |
| FKBP12 | FK506-binding protein 12 |
| FRB | FKBP12-Rapamycin-binding domain |
| mTOR | Mammalian target of rapamycin |
| GPCR | G protein-coupled receptor |
| $CB_1R$ | Cannabinoid-1 receptor |
| $D_2R$ | Dopamine $D_2$ receptor |
| $A_{2A}R$ | Adenosine $A_{2A}$ receptor |
| SH2 | Src homology 2 domain |
| OS-BLIA | Open sandwich bioluminescent assay |

| | |
|---|---|
| $V_H$ | Variable heavy chain of antibody |
| $V_L$ | Variable light chain of antibody |
| Trx | Thioredoxin |
| RT-PCR | Reverse-transcriptase polymerase chain reaction |
| ARM | Arginine-rich motifs |
| BIV | Bovine immunodeficiency virus |
| JDV | Jembrana deficiency virus |
| NIR | Near-infrared |
| QD/QDs | Quantum dot(s) |
| MMP-2 | Matrix metalloproteinase-2 |
| MMP-7 | Matrix metalloproteinase-7 |
| uPA | Urokinase-type plasminogen activator |
| CLuc | *Cypridina* luciferase |
| FBP | Far-red bioluminescent protein |
| Dlk-1 | Delta-like protein-1 |
| C-60 | Carbon-60/Fullerene |
| PMT | Photomultiplier tube |
| BLM | Bioluminescence microscopy |
| CCD | Charge-coupled device |
| EB-CCD | Electron bombarded charged coupled device |
| EMCCD | Electron multiplying cooled charge-coupled |
| DR | Double ratio |

## 10.1 Introduction

In this era of rapid expansion in scientific technology, scientists are keen on solving the mysteries of a variety of diseases. With more and more genomic data piling up, there is an urgent need to develop techniques that utilize this data to understand their phenotypic implications. Different biological processes are mediated by a plethora of specific protein-protein interactions (PPIs). Any anomalies in the genome will be manifested in the form of altered proteins and their functions. So, the study of these PPIs in normal and diseased cells becomes pivotal in the understanding of diseases and developing a suitable therapy. Conventional biochemical assays like coimmunoprecipitation [1, 2], gel-filtration chromatography [3], sandwich enzyme-linked immunosorbent assay (ELISA) [4], etc. have long been used in the investigation of PPIs. These assays, though successful, are essentially endpoint, in in vitro measurements and thus fail to provide spatiotemporal information on specific PPIs occurring within live cells. Furthermore, they also require mechanical-, chaotropic-, or detergent-based cell lyses, which can alter native PPIs in some cases [5, 6]. Moreover, such techniques are insensitive to transient interactions that may affect cellular processes. To overcome these limitations, various non-invasive approaches using genetic reporter genes

have been developed over the last two decades, which allow the study of PPIs in their native environment [6]. Of the various techniques developed, the yeast two-hybrid (Y2H) system [7], inducible yeast two-hybrid (IY2H) system [8], split reporter complementation assays or protein-fragment complementation assays (PCAs) [9], fluorescence resonance energy transfer (FRET), and bioluminescence resonance energy transfer (BRET) [6, 10] are prominent in the field. The Y2H uses a bait protein linked to a DNA-binding domain and is used to find a prey protein that is connected to a transcription activation domain. With a similar underlying principle, IY2H indicates an in vivo interaction under the influence of an external stimulus (e.g., cytokine, growth factor, etc.). The PCAs/split reporter complementation assays are based on the detection of a positive signal gain upon the reconstitution of the two functional halves of a reporter gene, usually an enzyme-like luciferase or $\beta$-lactamase, each of which are fused to potential protein partners of interest [6]. In contrast, BRET and FRET are biophysical techniques guided by the Förster Resonance Energy Transfer principle. In this chapter, we will be describing bioluminescence resonance energy transfer (BRET) principle in detail, highlighting various engineering aspects related to its assay design, customized development of various BRET-based sensors and ingenious advances in this technique in the recent past.

## 10.2 Biophysical Basis of BRET

### *10.2.1 Bioluminescence Light Emission*

Bioluminescence (BL), which is a naturally occurring phenomenon in many living organisms, has been used in the life sciences for several decades. Luminescence relies on an enzyme-based chemical reaction occurring within the specimen, and this enzyme–substrate catalysis results in the emission of a specific wavelength of light. This independent mechanism of light production has evolved in many organisms (especially in deep-sea organisms) to support their defense mechanism, distract predators, or even demonstrate sexual behavior [11].

The luciferases widely used in BRET are *Renilla* luciferase (RLuc) from the sea pansy *Renilla reniformis* and firefly luciferase (FLuc) from the firefly *Photinus pyralis*. Other luciferases that have been introduced as candidates for BRET include *Gaussia*, *Metridia,* and *Vargula* luciferases (discussed later in this chapter). The exact mechanism for bioluminescence reactions differs from species to species. However, they are broadly categorized into two groups as ATP-dependent and ATP-independent reactions. The first group comprising of beetle firefly luciferases (FLuc) requires ATP and $Mg^{2+}$ for the catalytic reaction. During this reaction, FLuc enzyme catalyzes the production of luciferyl adenylate ($LH_2$-AMP) from the substrate D-luciferin ($LH_2$) in the presence of ATP. Then, $LH_2$-AMP is oxidized by molecular oxygen to yield excited-state oxyluciferin and $CO_2$.

The excited-state oxyluciferin relaxes to its ground state with the emission of yellowish green light (emission maximum or $Em_{max}$ 562 nm) and AMP [12–15]. This ATP dependency has been widely used as a method to determine the cellular ATP levels in bacteria and blood [16].

On the other hand, luciferases such as RLuc that use imidazopyrazinone-type substrate called coelenterazine (Clz) function in an ATP-independent mechanism that employs a simple oxygenation reaction, wherein $O_2$ is incorporated into the RLuc substrate to form an excited state intermediate dioxetane derivative that releases $CO_2$, followed by the formation of an excited coelenteramide anion that ultimately yields a photonic blue light emission ($Em_{max}$ 480 nm) [14, 17].

### *10.2.2 Fluorescence Light Emission*

In a fluorescence emission, electrons in the fluorophore get excited upon illumination by an excitation light source in the UV or visible range. In this excited state, the electrons dissipate some of their excess energy through collisions with other molecules. The fluorophore then relaxes back to its ground-state energy level by emitting low-energy photons at a wavelength longer than the excitation photons [18]. Different fluorophores have distinct excitation and emission spectra which can be detected using specific filter sets of appropriate wavelength range.

### *10.2.3 Förster Resonance Energy Transfer*

Resonance energy transfer (RET) is a principle that was first described by the German scientist Theodor Förster in 1948 to describe the quantum–mechanical behavior of the transfer of electronic excitation energy between two molecules. Basically, RET is a phenomenon occurring between two closely spaced chromophores (color-producing compounds) when the emission spectrum of one (the donor) overlaps with the excitation spectrum of the other (the acceptor). Following donor excitation, part of the electronic excitation energy of the donor is dissipated due to random collisions with other molecules, while the remaining electronic relaxation energy is transferred to the acceptor molecule through non-radiative dipole–dipole coupling [19]. It is important to understand here that transfer of resonance energy between the donor and acceptor does not take place in the form of a physical entity like photons. It is simply an electrodynamic interaction or non-radiative energy which occurs between the electric fields of the transient dipoles of the donor and the acceptor [20]. Upon excitation, the acceptor molecule now acts as a normal fluorophore and emits its photonic energy at its characteristic wavelength (Fig. 10.1). This results in a decrease in donor emission paralleled by an increase in acceptor emission [10]. Thus, the secondary emission by the acceptor molecule is the outcome of the energy transfer only and not from any external light source.

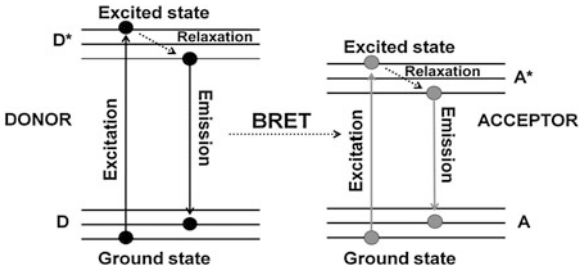


**Fig. 10.1** Jablonski diagram to illustrate the electronic changes occurring in the donor and acceptor molecules during a BRET process. The donor (*D*) molecule is normally in its ground state energy level. Upon substrate oxidation, it is elevated to a higher energy state (*D**). Then, the excited donor loses some of its energy as vibrational relaxation energy. A part of the remaining energy is either emitted out as donor luminescence or is transferred to the nearby acceptor in a non-radiative manner. The acceptor fluorophore now gets excited (*A**) and then relaxes back to its ground state by releasing photons at its characteristic wavelength, completing a BRET process

### *10.2.4 Factors Controlling Energy Transfer in RET*

Several variables affect the efficiency of energy transfer between the two chromophore groups. First, the distance between the donor and acceptor molecule which is inversely proportional to the extent of energy transfer; the energy transfer gradually decreases when the distance between the donor and acceptor increases. The optimal distance for Förster resonance energy transfer is 1–10 nm. This is because the efficiency of energy transfer ($E_{\mathrm{RET}}$) is inversely proportional to the sixth power of the distance ($R$) between donor and acceptor molecules, Eq. 10.1.

$$E_{\mathrm{RET}} = \frac{1}{1 + \frac{R^6}{R_0}} \tag{10.1}$$

where $R_0$ is the distance for 50 % energy transfer from the donor to the acceptor, which is about 5 nm [10, 21, 22]. Now, the Förster distance of a pair depends on the overlap integral of the donor emission spectrum with the acceptor absorption spectrum and their mutual molecular orientation and is calculated based on the Eq. 10.2.

$$R_0 = 2.11 \times 10^{-2} \times \left[\kappa^2 \times J(\lambda) \times \eta^{-4} \times Q_D\right]^{1/6} \tag{10.2}$$

where $\kappa^2$ is the dipole orientation factor, $\eta$ is the refractive index of the medium, $J(\lambda)$ is the spectral overlap integral, and $Q_D$ denotes the donor quantum yield in the absence of acceptor. Because of the sixth-root dependence in the calculation of $R_0$, small changes in the value of $Q_D$ should not have a large effect on the overall BRET efficiency [23, 24]. Second, the orientation angle between donor and acceptor molecules affects RET efficiency since energy transfer will take place only if the transient dipoles of the interacting molecules are aligned in a position suitable for this transfer. Third, the degree of spectral overlap between donor emission and acceptor absorbance is also a significant factor. Higher the spectral overlap, the better the energy transfer [22]. Fourth, the quantum yield of the donor

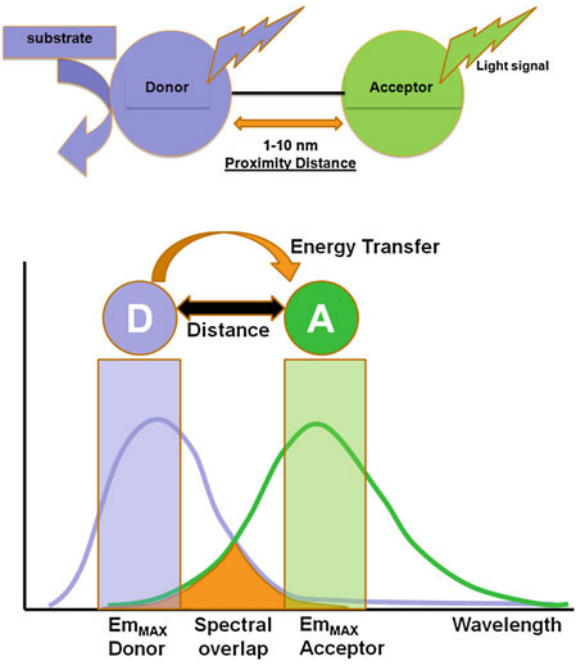


**Fig. 10.2** Schematic illustration of the basic elements involved in a typical BRET system. In the presence of its specific substrate, the donor luciferase gets excited and emits light at its characteristic wavelength. Within the proximity distance of 1–10 nm, resonance energy transfer occurs to a suitable fluorescence acceptor, leading to the photon emission at its characteristic wavelength. Light signal obtained from both donor and acceptor emission can be measured using suitable band-pass filters, and BRET ratio can be judged as a measure of the distance between the donor and acceptor pair

should be high, since the energy cannot be transferred if it is lost too quickly through non-radiative decay [6].

In the RET-based PPI assay, i.e., BRET or FRET, the two chromophores are genetically tagged to two proteins whose interaction is to be investigated. The strict dependence of RET on the inter-chromophoric distance (1–10 nm) makes it an appropriate "molecular yardstick" for determining PPIs. This is true, since the average protein radius is ~5 nm, which means that a positive RET signal will only take place if the two proteins come within ~10 nm of each other, a distance that is an indicator of direct interaction between the two proteins [21].

### *10.2.5 Bioluminescence Resonance Energy Transfer*

BRET exploits non-radiative (dipole–dipole) energy transfer occurring between a luminescent luciferase donor (instead of a fluorescent donor as in FRET) and a compatible fluorescent protein (FP) acceptor in order to study PPIs between two proteins fused to these donor and acceptor moieties (Fig. 10.2). The detection of a positive BRET signal means that the two proteins are situated within the BRET-permissive distance of 10 nm, thereby positively affirming their interaction [25, 26]. However, absence of a BRET signal does not necessarily mean that the two target proteins do not interact with each other. Lack of a signal can be accounted for by an unfavorable orientation between the donor and acceptor dipoles [27]. To nullify this

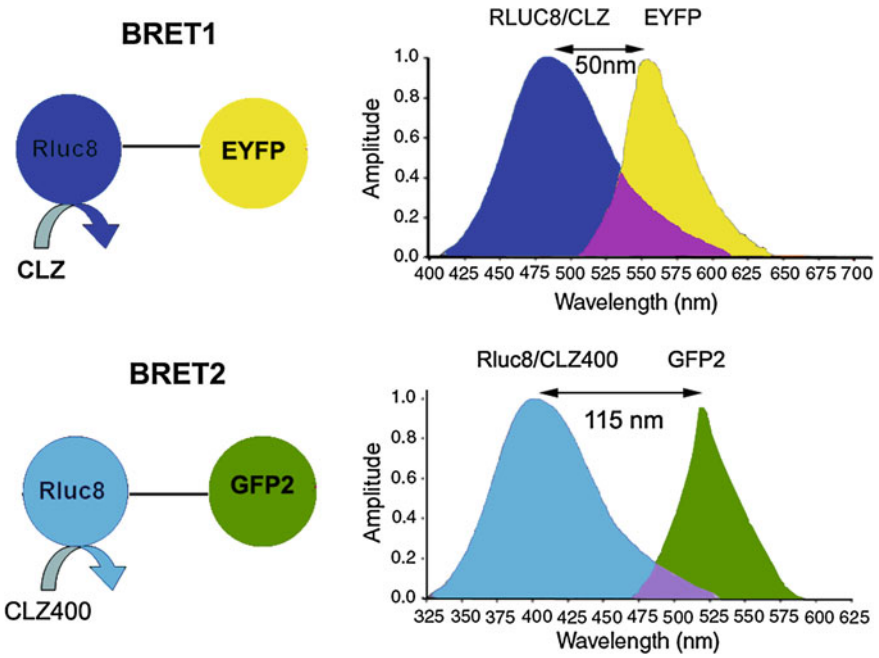


**Fig. 10.3** Schematic representations of $BRET^1$ and $BRET^2$ assays showing all the essential components in each. While both $BRET^1$ and $BRET^2$ use RLuc donor, they use different coelenterazine analogs such as Clz and Clz400 as indicated. Note the change in donor emission maximum in case of $BRET^2$. In general, an 18-amino-acid linker is placed between the donor and acceptor proteins. Spectral resolution of each system is marked as a bidirectional arrow and spectral overlap region is marked with purple-color zone at the intersection of the donor and acceptor emission. Note, the donor and acceptor emission spans and intensities are thematic (not normalized)

issue, both N- and C-terminus fusions using flexible peptide linkers (6–18 amino acids) must be tested. Such design can reduce steric hindrance and improve the orientation. Normally, the linker sequence comprises of GGGGS or (GGGGS) × 2 residues where glycine–serine combinations confer flexibility, allowing the fusion proteins to fold to their optimal conformation [28, 29] and achieve the proximity distance between donor and acceptor.

BRET is an intrinsic phenomena occurring in the organisms *Renilla reniformis* and *Aequorea victoria.* In *Aequorea victoria,* a $Ca^{2+}$-dependent photoprotein called aequorin releases flashes of blue light, which is transduced by a green fluorescent protein (GFP) to emit green light. Exploiting the underlying principle of BRET from *Aequorea victoria*, Xu et al. developed a BRET system in 1999 to study the interactions of circadian clock proteins in bacteria [25]. This BRET system termed as $BRET^1$ uses *Renilla* luciferase (RLuc) as the donor moiety and enhanced yellow fluorescent protein (EYFP) as the acceptor ($Em_{max} \sim 530$ nm) moiety. The spectral resolution (separation of peak donor and acceptor emission spectra) achieved in $BRET^1$ is ∼50 nm only (Fig. 10.3) [23, 30].

Another BRET system, designated as BRET$^2$ was developed that combined RLuc with a UV-excitable GFP variant called GFP$^2$ [31, 32]. In this case, the substrate for RLuc was a coelenterazine analog DeepBlueC$^{TM}$ (also known as coelenterazine 400a/Clz400, bisdeoxycoelenterazine), which is similar to the native substrate in being cell permeable and non-toxic but shifts the $Em_{max}$ to 400 nm. GFP$^2$ excites at a maximum ($Ex_{max}$) of 396 nm and emits photons at 510 nm. This yields a much larger spectral resolution of 110 nm (Fig. 10.3), which allows the use of wideband filters and minimizes bleed-through signal (residual emission of RLuc detected by the acceptor filter or vice versa). On the other hand, possible disadvantages associated with the use of the Clz400 substrate are poor substrate utilization, reduced quantum yield ($\sim$100 fold lower than Clz), and rapid decay in serum [23, 27]. Seeing the above two examples, it becomes clear that the balance between quantum yield and spectral resolution is of critical importance while choosing an appropriate BRET pair for in vivo applications. One should bear in mind that the same factors that affect the efficiency of RET are also applicable in BRET. To design the required BRET fusion proteins, the cDNA of the target proteins is inserted in frame into a suitable expression vector (by placing an appropriate linker as mentioned before) that has either the donor or acceptor gene. The stop codon of the amino terminus protein of the fusion partner should be removed by mutagenesis, and it should only be present in frame at the end of the carboxyl terminal protein so that the fusion protein can be expressed. One can design both C- and N- terminal protein fusions to assess their efficacy. Once the required fusion proteins are verified by expressing in mammalian cells, the BRET signal can be measured using suitable filter sets as explained later in this chapter. The BRET ratio [33] can be calculated as per Eqs. 10.3 and 10.4.

$$\text{BRET} = \frac{\text{BL}_{\text{emission}}(\text{Acceptor}) - C_f \times \text{BL}_{\text{emission}}(\text{Donor})}{\text{BL}_{\text{emission}}(\text{Donor})} \tag{10.3}$$

where

$$C_f = \frac{\text{BL}_{\text{emission}}(\text{Acceptor})_{\text{donor-only}}}{\text{BL}_{\text{emission}}(\text{Donor})_{\text{donor-only}}} \tag{10.4}$$

In Eq. 10.4, the correction factor ($C_f$) represents the BRET signal detected from cells transfected only with the donor protein. Subtracting this factor from the overall BRET ratio can give us an idea of the dynamic range for a particular BRET pair. Moreover, since BRET-based assays can be performed on live cells, under normal culture conditions and the indicative result being ratiometric, any variability due to assay volume or cell number variation is nullified.

## 10.3 Engineering the BRET Components

So far, we have just begun to understand the basic principles underlying the BRET technique. In order to explore the engineering aspects of BRET, we need to delve deeper into four main facets viz., the donor components i.e., the luciferase protein and its substrate, the acceptor fluorescent protein as well as detection devices (discussed in Sect. 10.5).

### *10.3.1 Bioluminescence Donor*

As indicated before, to date, the luciferase enzyme from *Renilla* sp. has been predominantly used as the donor protein for the BRET systems in use, but in the recent years, several other luciferases from various other sources have also been engineered and used as BRET donors. We will now discuss various aspects of protein engineering that have been applied to each of them. Simultaneously, where applies, their respective engineered substrate is also discussed.

#### 10.3.1.1 *Renilla* Luciferase and Coelenterazine

The main strength of a BRET signal is primarily dependent upon the efficiency of the luciferase enzyme to yield a high photon output upon the oxidation of its substrate. The 35-kDa RLuc protein typically emits light in the blue-green region ($Em_{max}$ 480 nm). To further increase the donor quantum output, Angers et al. used coelenterazine-h (Clz-*h*) as a substrate for RLuc, which has the same $Em_{max}$ as native Clz, but has a higher luminescence capacity than the latter [34]. For usage of this luciferase enzyme in mammalian systems, predominantly human cell lines, several commercial sources have developed a codon-optimized version hRLuc (BioSignal Packard) or hRL (Promega) that display improved bioluminescence than the native protein. However, a major limitation of hRLuc is its poor stability in serum (half-life of $\sim$0.5–1 h in murine serum) which impedes bioluminescence or BRET imaging in animals for a sustained time period. To correct this problem, Loening et al. adopted a consensus-guided mutagenesis approach (for details, refer to Chap. 8) to identify beneficial mutations in hRLuc that render increased stability to the enzyme [35]. In the process of doing so, they also pinpointed mutations that showed increased quantum output. Upon introducing various point mutations, RLuc2 (C124A, M185V) and an eight mutation form of RLuc i.e., RLuc8 (A55T, C124A, S130A, K136R, A143M, M185V, M253L, and S287L) were developed that displayed greatly improved characteristics suitable for developing new BRET partners. Compared with the native enzyme, RLuc8 exhibited an intracellular half-life >50 h, a fourfold increment in quantum output, and a 5-nm wavelength shift in the emission spectrum [35]. The successful utilization of these mutations in

improving $BRET^2$ assay sensitivity with expanded dynamic range was demonstrated by us [24]. Later, by combining RLuc8 with the monomeric red FP variant mOrange ($Em_{max}$ 564 nm), the BRET3 system was also developed (Fig. 10.4). On addition of Clz substrate, BRET3 provides a spectral resolution of ~85 nm [30]. Further, RLuc8 has shown to transfer adequate energy over a spectral distance of 100 nm when we combine RLuc8 donor with TagRFP ($Em_{max}$ 584 nm) [36].

Another obstacle to the use of RLuc and its variants in BRET imaging was the blue-green light emission that greatly attenuated the signal in animal tissues, as pigments like myoglobin and hemoglobin strongly absorb photons from the blue-green region. Thus, use of RLuc for BRET detection from deeper tissues was severely limited [30, 37]. In the field of in vivo imaging, it is well known that light emitted above 600 nm can be better detected from deeper tissues of small animals. To achieve red-shifted light emission from RLuc, efforts have been made in two possible ways, i.e., genetic engineering of luciferase protein itself and chemical engineering of Clz substrate. Applying the genetic engineering approach to produce more red-shifted RLuc, Loening et al. [38] identified several mutants of which RLuc8.6 with an $Em_{max}$ 535 nm (A123S, D154M, E155G, D162E, I163L, V185L point mutations in RLuc8) showed significant promise in live cells as well as animals. In 2010, Loening et al. [39] created another variant i.e., RLuc7 ($Em_{max}$ 521 nm) with a rapid turnover and a half-life (~6.8 h) similar to the native RLuc in order to detect transient changes in gene expression. RLuc7 exhibited a twofold increase in the signal output compared to RLuc. Depending on the experimental requirements, one can decrease the stability of the luciferase enzyme without any mutagenesis by simply appending a signaling sequence at the 5′ or 3′ termini of the protein to direct the protein to early degradation. One such sequence is the PEST (Pro-Glu-Ser-Thr) sequence that has been frequently used to produce destabilized luciferases [40, 41].

Another remarkable finding is that the utilization of coelenterazine analog Clz-*v* with any of the RLuc variants has an additive effect as it further shifts the $Em_{max}$ to the right by 35 nm. As shown, by using Clz-*v* in combination with RLuc8.6 protein, one can obtain an $Em_{max}$ at 570 nm [36]. However, this substrate is not commercially available because of its problematic purification process possibly owing to sensitivity under chromatographic conditions, and it exhibits an order of magnitude increase in background auto-chemiluminescence [39]. Stepanyuk et al. ligated Clz-*v* to the coelenterazine binding protein (CBP) from the organism *Renilla muelleri* which acts as a 'protector' for Clz-*v* that results in a marked improvement in the stability of this conjugated Clz-*v* at 37 °C in addition to a higher bioluminescence signal output (twofold) in comparison with the native Clz-*v* when used with a *R. muelleri* luciferase (RLuc-m) mutant [42]. Taking advantage of these mutated RLuc donor and Clz analogs, several new combinations of BRET using red and far-red FPs have also been made as summarized in Fig. 10.4, expanding the scope of multiplexed BRET imaging. Of these new assays developed, BRET8 displaying a spectral resolution of 100 nm was used to image live cells and animals in the far-red region of the visible spectra [36]. Point to be mentioned, in Fig. 10.4, we have renamed some of the recently developed

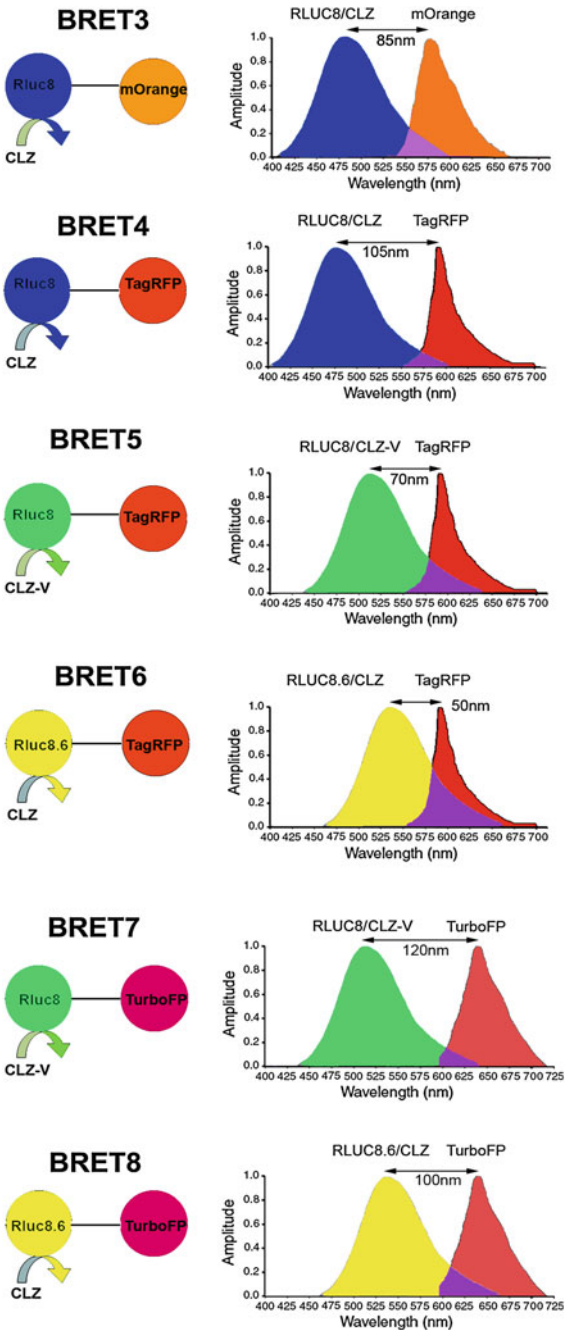


**Fig. 10.4** Schematic representation of the expanded BRET fusion constructs developed using *Renilla* luciferase donor. The bioluminescence spectra illustrate the emission spectra of the RLuc mutants used as donor and the emission of the red fluorescent acceptor proteins. For all constructs, an 18-amino-acid linker is used between the donor and acceptor proteins. Luciferase substrates used in each case are indicated as either CLZ or CLZ-*v*. Spectral resolution of each system is marked as a bidirectional arrow. Spectral overlap region is also marked with a purple-color zone at the intersection of the emission spectrum. Note, the donor and acceptor emission spans and intensities are thematic (not normalized). Figure adapted with modifications as permitted by PNAS [36]

BRET vectors, such as BRET4.1, BRET5, and BRET6 as BRET5, BRET6, and BRET8, respectively, while eliminating some others reported such as BRET3.1 or BRET6.1 as their low spectral resolution may impede spectral separation for BRET imaging application.

Efforts continued further on synthesis of new coelenterazine analogs with better bathochromic emission shifts. Recently, Giuliani et al. [43] developed a new series of red-shifted coelenterazine analogs and a novel approach to alter the photochemical properties of the light-emitter intermediates. By insertion of a C-8-bonded S atom, the substrate molecules favor the emergence of lower energy emitters in coelenteramide. This bathochromic effect was evident in the presence of either the phenyl or the phenol ring in C-6, indicating that the red-shift can occur regardless of whether the main emitter is the neutral or the amide–anion form of the molecule.

One problem associated with coelenterazine and its derivatives was its quick decay upon auto-oxidation in the presence of aqueous media of cultured cells. For instance, Clz reduces in concentration by 50 % within 17 min of its addition to cell media. This decay not only reduces the availability of Clz molecules in the media, but also increases the background signal, thereby decreasing the assay sensitivity. Moreover, this limits its use in BRET assays to cell lysates only and fails to empower BRET applications to catch the live cell dynamics. This is equally true for other Clz analogs including Clz400. To solve this problem, Levi et al. [44] reported a clever approach to protect the putative oxygenation sites of Clz400 substrate and demonstrated that depending on the protection modifications, long-term $BRET^2$ monitoring is achievable. Similarly, another commercial source has developed two substrates EnduRen™ and ViviRen™ that can be used specifically for live cell imaging [45]. These are protected forms of coelenterazine that have esters or oxymethyl ethers added at the site of substrate oxidation. The intracellular esterases and lipases yield the active Clz-*h* upon hydrolytic cleavage of the protected forms. The absence of active Clz-*h* in the media significantly reduces the background signal due to auto-oxidation, and the half-life of Clz-*h* increases. EnduRen™ and ViviRen™ substrates have been designed to display different kinetics. EnduRen™ shows a slow but gradual increase in bioluminescence. It reaches its maximum photon output at 90 min and then emits a constant signal for over 24 h (Fig. 10.5). In contrast, ViviRen™ can generate a threefold brighter signal which is instantaneous but short-lived. Pfleger et al. [46] demonstrated the use of EnduRen™ in monitoring the agonist-induced interaction of GPCRs in real time over a period of several hours. This was the first successful step in the direction of real-time BRET assays, as previously, the short half-life of Clz-*h* hampered the monitoring of PPIs in live cells. This modified BRET system was designated as extended BRET (eBRET), which is a superior approach for dynamic monitoring of PPI kinetics in their native cellular environment.

#### 10.3.1.2 Firefly Luciferase and D-Luciferin

Another commonly used luciferase is the North American firefly luciferase (FLuc) from *Photinus pyralis*. It is a 61-kDa protein that emits orange light at an $Em_{max}$

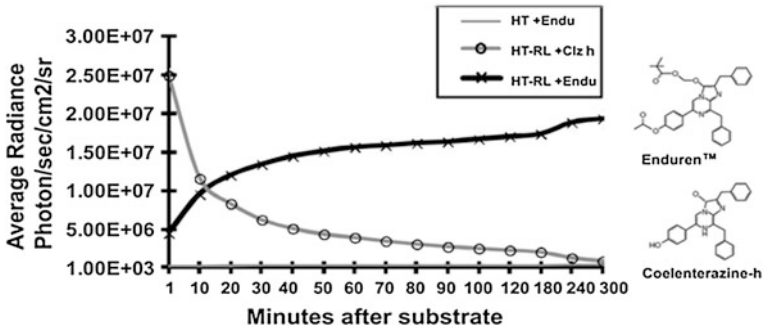


**Fig. 10.5** Chart represents time kinetics of the light output after addition of normal coelenterazine-*h* substrate or protected coelenterazine-h substrate i.e., EnduRen™ [45]. Plain HT1080 mammalian cells (HT) or HT1080 cells overexpressing RLuc8 protein (HT-RL) were used for measuring the photon output as marked. Note the difference of time kinetics, where Clz-*h* substrate activity diminishes quickly within an hour; EnduRen™ substrate activity shows gradual increase till 90 min and remains maintained till the end point of measurement. Also note the *y*-axis scale bar representing a log scale. Note changes in the chemical structures that convert the Clz-*h* substrate into EnduRen™

562 nm [47, 48]. The emission of orange bioluminescence is a positive feature for bioluminescence imaging (BLI); however, its use in BRET is limited thus far, owing to its bulky size and low photon output. Moreover, the obligate dependence of FLuc on $Mg^{2+}$ and ATP as its cofactors also diminishes its worth as a BRET donor. Nonetheless, FLuc has been employed in several BRET applications in combination with red- and far-red-shifted FPs such as DsRed [49] and mKate variant [50], respectively, as well as non-protein fluorophores [51]. For example, Arai et al. reported the use of the coral red fluorescent protein (DsRed) ($Ex_{max}$ 558 nm; $Em_{max}$ 583 nm) as acceptor in combination with FLuc [49]. However, the use of DsRed is not preferred owing to its propensity to tetramerize, and the FLuc-DsRed system will have a spectral resolution of <20 nm which is highly unfavorable due to substantial overlap between FLuc and DsRed emission peak, thus necessitating the use of signal correction factor. Recently, BRET comprising a thermostable mutant form of firefly luciferase from *Photinus pyralis* (Ppy WT-TS; $Em_{max}$ 565 nm) along with a variant of mKate (S158A) ($Em_{max}$ 610 nm) was developed by Branchini et al. [52]. In the literature, Cy3 and Cy3.5 fluorophores have been attempted to be combined with FLuc as BRET partners [51]. However, the main drawback of using a non-protein fluorophore is that it has to be chemically linked with the donor and must be efficiently delivered within the cell for signal detection. Taking all these factors into account, the use of FLuc in BRET systems still needs to be optimized. Similar to RLuc, the codon-optimized version of FLuc (hFLuc) for use in mammalian cells has been created by commercial sources. Caysa et al. [37] have developed a red-shifted mutant of hFLuc ($Em_{max}$ 615 nm) by introducing a single point mutation S284T. Even though the light output of the mutant FLuc drops to 25 % of the native FLuc, the signal output detected from whole animals is considerably higher (threefold) than its native

counterpart, possibly due to the reduced tissue attenuation attributed to the red-shift in emission to above 600 nm. Branchini et al. [53] have also developed several FLuc mutants Ppy GR–TS and Ppy RE–TS that possess an $Em_{max}$ of 546 and 610 nm, respectively, and Ppy RE8 and Ppy RE9 that show an $Em_{max}$ of 617 nm, with Ppy RE9 being the superior luciferase. However, to the best of our knowledge, these mutant forms have so far not been recruited in any BRET system. In the D-luciferin molecule, N- and S-heteroatoms exist in a particular electron-rich configuration, which may play a fundamental role in the formation of multiple oxyluciferin excited states, resulting in a relatively broad emission spectrum [54]. Furthermore, the relatively slower and stable emission kinetics makes it naturally suitable for kinetic measurements from live environment without chemical modifications to its structure.

#### 10.3.1.3 Other Luciferases

A range of other luciferases are now available from organisms like *Metridia longa*, *Metridia pacifica*, *Cypridina noctiluca*, *Oplophorus gracilirostris*, click beetle, railroad tapeworm (*Phrixothrix hirtus*), *Vargula hilgendorfii*, *Gaussia princeps*, etc., most of which are marine organisms. Some of them are popularly used as reporter genes for BLI, but have limited applicability in BRET due to their undesirable characteristics. For instance, M*etridia* luciferases (MLuc) are secretory in nature [55, 56], while *Oplophorus* luciferase (OLuc) is a 106-kDa secretory protein composed of a dimeric repeat [57] which is too bulky for use in BRET. Some luciferases show promising features and have successfully been exploited in the development of functional BRET systems. These comprise of click beetle green luciferase (CBG) [58], *Gaussia* luciferase (GLuc) [59], and *Vargula* luciferase (VLuc) [60].

Gammon et al. [58] reported a new combination of click beetle green (CBG) luciferase as donor and tdTomato as acceptor. *Gaussia* luciferase (GLuc) is a 19.9-kDa secretory protein with an $Em_{max}$ 480 nm that extends till 600 nm. A codon-optimized version of GLuc (hGLuc) offers several advantages over other luciferases. In addition to its small size, hGLuc is highly heat stable, strongly resistant to acidic and basic conditions, and generates a $\sim$100-fold higher intracellular signal compared to FLuc and hRLuc. Furthermore, unlike hRLuc or FLuc, it can be used either as a secretory or as an intracellular reporter depending on the experimental needs [61]. These features can contribute to the robustness of GLuc-based BRET systems. Li et al. reported the development of GLuc-EGFP BRET assay for protease activity sensing in in vitro [59]. Like GLuc, *Vargula* luciferase (VLuc) is a secretory protein, but of higher size (62 kDa) [62] with an $Em_{max}$ 460 nm. The VLuc-EGFP combination has been reported by Otsuji et al. [60]. Irrespective of its bulky size, this system offers similar benefits in terms of applicability as in GLuc.

NanoLuc$^{TM}$ (NLuc) is a mutant form obtained from the deep-sea shrimp *Oplophorus* luciferase (OLuc). OLuc is a heteromeric structure composed of two

19-kDa catalytic subunits (OLuc-19) and two 35-kDa subunits (OLuc-35) that provide stability to the 19-kDa subunits. When Inouye et al. attempted to use the isolated OLuc-19 as a luciferase, they found that it was highly unstable and poorly expressed in the absence of its 35-kDa counterpart [57]. Hall et al. envisaged the creation of a variant of this OLuc-19 that ultimately led to the generation of NLuc. To achieve this, OLuc-19 was subjected to site-directed and random mutagenesis in order to obtain a stable variant. Further, through a single round of random mutagenesis, they generated a variant C1A4E with eight mutations (A4E, Q11R, A33K, V44I, A54F, P115E, Q124K, and Y138I). In the next phase, several coelenterazine derivatives were screened in order to create a superior substrate for optimal bioluminescence. Twenty-four coelenterazine analogs were developed and then screened against a library of C1A4E variants. Of these, the C1A4E variant (Q18L, F54I, F68Y, L72Q, M75K, and I90V) showed a $\sim$10-fold higher stability over C1A4E at 37 °C with the coelenterazine derivative 2-furanylmethyl-deoxy-coelenterazine (Furimazine). In the final phase of optimization, they used furimazine to screen for other beneficial mutations in OLuc-19 variants. These mutations (L27V, K33N, K43R, and Y68D) were then combined with the previous mutations to produce NanoLuc™. In total, 16 amino acid substitutions of the wild-type OLuc-19 resulted in NLuc, having $Em_{max}$ 460 nm and an intracellular half-life of >15 h at 37 °C. Using furimazine as its substrate exhibits a >150-fold higher light output than both RLuc and FLuc, which makes it a very attractive candidate for BRET multiplexing. Despite the emission maxima of NLuc in the blue-green region, its sufficiently high quantum output with furimazine can be used to couple it with any of the available BRET acceptors currently used with RLuc8.

### *10.3.2 Fluorescence Acceptor*

The other component of a BRET system is a fluorescent protein that can be compatibly partnered with the luciferase in use. A good FP entails several characteristics. First, it should express efficiently in a system without invoking any cellular toxicity. Second, it should produce a high signal-to-noise ratio. Third, the FP should have sufficient photostability so as to be imaged for the duration of the experiment. Fourth, if the FP is to be fused to another protein of interest, then it should not have a tendency to oligomerize. Finally, it should be resistant to environmental conditions like pH and temperature [63].

Having realized the versatility of FPs in a variety of biological applications such as imaging and FRET, wild-type GFP from the organism *Aequorea victoria* (also known as wtGFP or avGFP) isolated by Shimomura et al. was cloned by Prasher et al. in 1992 [64]. Thus began the era of "GFP-technology". The chromophore of wtGFP consists of Ser/Thr65-Tyr66-Gly67, which is protected by a shell consisting of 11 strands of $\beta$-barrels and one $\alpha$-helix. The N- and C-termini of GFP are flexible, whereas the $\beta$-barrel shell is well structured and rigid, which protects the chromophore group from the external environment [65]. However, it

does not fold efficiently at 37 °C since the optimal temperature for its maturation is 28 °C [66], and it forms weak dimers that may result in the formation of artifacts [65]. Thus, several GFP variants have been created, of which EGFP (Enhanced GFP from Clontech), AcGFP (Clontech), TurboGFP (Evrogen), and Emerald (Invitrogen) have overcome some of the limitations of GFP.

Yellow fluorescent proteins (YFPs) provide an edge over GFPs as their emission maxima lies in the 500–550 nm range. The original enhanced yellow fluorescent protein (EYFP) was derived from wtGFP and is now obsolete owing to its high sensitivity to chloride ions and slower maturation at 37 °C. Overcoming this problem, several successors of EYFP are now available such as citrine and its monomeric version mCitrine [67], Venus [68], and YPet [69]. Of these, YPet displays the brightest signal and so provides an advantage over its competitors [69].

As discussed above, a major shortcoming of using GFPs or YFPs used in early generation of BRET assays is their photon attenuation in mammalian tissues. To fulfill this demand of FPs emitting at red and far-red range, screening of various animal resources was initiated. A major breakthrough was the isolation of DsRed—a red fluorescent protein (RFP) from coral *Discosoma striata*. The excitation and emission maxima of DsRed are at 558 and 583 nm, respectively [70]. Moreover, it exhibits several positive features such as elevated extinction coefficient, high quantum yield, resistance to pH variations, and resistance to photobleaching. DsRed, however, tends to form tetramers [71], which often results in the poor localization as well as artificial oligomerization that may consequently impair the functions of proteins to which it is tagged. Furthermore, this chromophore matures very slowly, often taking days for the protein to convert from the premature greenish to the mature red emission. Monomeric RFP1 (mRFP1) [72] obtained after multiple rounds of mutagenesis (33 mutations in the parental DsRed) was the first true monomeric RFP with distinct improvements over previous versions of DsRed, namely DsRed2, T1 [73] and dimer2 [72], such as faster maturation and a 25-nm wavelength shift in excitation and emission. However, mRFP1 failed to acquire images with high spatial and temporal resolution due to its much lower quantum yield and extinction coefficient and a poor photostability [72]. Overcoming these limitations, Shaner et al. [74] and Wang et al. [75] reported a wide range of monomeric 'fruit' FPs named after fruits, representing the color similar to their emission such as mHoneydew, mBanana, mOrange, mTangerine, mStrawberry, mCherry [74], mRaspberry, and mPlum [75], as well as a tandem dimeric FP tdTomato, all with relatively long excitation and emission wavelengths (Table 10.1).

Another group, Merzlyak et al. [76], developed RFP variants from a red eqFP578 protein isolated from the sea anemone *Entacmea quadricolor*. Dimeric eqFP578 again underwent several rounds of random mutagenesis that consequently produced an enhanced dimeric FP called TurboRFP with $Em_{max}$ 574 nm. TurboRFP displayed superior qualities over DsRed2 such as greater pH stability, faster maturation at 37 °C, and higher extinction coefficient and quantum yield. Despite being a dimer, TurboRFP does not form aggregates in cell. It was further subjected to site-directed mutagenesis (R162E, Q166D, S180N, F198V, and F200Y) that contribute to the dimeric nature of TurboRFP as well as random

**Table 10.1** The key properties of various classes of fluorescent proteins

| Class | Fluorescent protein | $Ex_{max}$ (nm) | $Em_{max}$ (nm) | Oligomerization | Reference |
|---|---|---|---|---|---|
| Green | GFP | 395/475 | 508/503 | w.d. | [80] |
| | EGFP | 488 | 507 | w.d. | [80] |
| | Emerald | 487 | 509 | w.d. | [80] |
| Yellow | EYFP | 514 | 527 | w.d. | [63] |
| | Venus | 515 | 528 | w.d. | [68] |
| | mCitrine | 516 | 529 | m.m. | [67] |
| | YPet | 517 | 530 | w.d. | [69] |
| Orange | mBanana | 540 | 553 | m.m | [74] |
| | mKO | 548 | 559 | m.m. | [81] |
| | mOrange | 548 | 562 | m.m. | [74] |
| Red and Far-red | TurboRFP | 553 | 574 | d.m. | [76] |
| | tdTomato | 554 | 581 | t.d. | [74] |
| | DsRed | 558 | 583 | t.m. | [70] |
| | TagRFP | 555 | 584 | m.m. | [76] |
| | mTangerine | 568 | 585 | m.m. | [74] |
| | mStrawberry | 574 | 596 | m.m. | [74] |
| | mCherry | 587 | 610 | m.m. | [74] |
| | mRaspberry | 598 | 625 | m.m. | [75] |
| | mKate2 | 588 | 633 | m.m. | [78] |
| | mKate | 588 | 635 | m.m. | [77] |
| | TurboFP635/ Katushka | 588 | 635 | d.m. | [77] |
| | mPlum | 590 | 649 | m.m. | [75] |
| | TagRFP657 | 611 | 657 | m.m. | [79] |

*w.d.* weak dimer, *d.m.* dimer, *m.m.* monomer, *t.d.* tandem dimer, *t.m.* tetramer

mutagenesis to stabilize the monomeric form. The final product obtained was TagRFP which is a monomer and has a 10-nm shift in its $Em_{max}$. In addition, it is almost 2–3 folds brighter than mCherry, with a good maturation rate and a very high pH stability ($pK_a = 4$), making it suitable for use in acidic organelles as well. Furthermore, Shcherbo et al. [77] succeeded in generating a dimeric RFP called Katushka or TurboFP635, with excitation and emission peaks at 588 nm and 635 nm, respectively. It is characterized by fast maturation rate, high pH stability ($pK_a = 5.5$), low toxicity in mammalian cells, and superior brightness in comparison with its counterparts in the 650–800 nm optical window. However, since Katushka was dimeric in nature, Shcherbo et al. also targeted to develop monomeric Katushka, called mKate. They used monomeric TagRFP as the starting template and modified the residues surrounding its chromophores group to resemble that of Katushka. Thus, mKate has similar spectral characteristics as Katushka, albeit with slightly lowered quantum yield and pH stability. Shcherbo et al. [78] further optimized mKate and developed mKate2. Adding the mutation S165A to mKate, which converted its crystal structure from the *trans* to the *cis* form, resulted in an mKate variant with higher brightness and lower pH dependence. They also added two beneficial mutations V48A and K238R, developing

the final product mKate2 with enhanced brightness and improved pH stability, photostability, and maturation rate. It is threefold brighter than mKate and 10-fold brighter than mPlum. Morozova et al. [79] have also recently succeeded in developing an even further red-shifted variant of mKate called TagRFP657 with $Ex_{max}$ and $Em_{max}$ at 611 and 657 nm, respectively.

## 10.4 Engineering BRET Sensors for Functional Measurement

Unlike many other assays such as PCA, BRET system provides unique opportunity to readily adapt the newly evolved donor and acceptor proteins with preferred characteristics. This feature of BRET led to the rapid expansion and growth in identifying new BRET formats which eventually widened the BRET applicability. In this section, we will focus on engineering efforts that have expanded the scope of BRET applications. To do this, we can categorize reports under two major subheadings i.e., genetic BRET systems and synthetic BRET systems and discuss various applications that they have been tested for.

### *10.4.1 Genetic BRET Systems*

As stated above, several genetically encoded BRET systems comprising of different combinations of luminescent and FP variants have been developed over the last decade. Due to attenuation of photons below 600 nm wavelengths in biological tissues, the $BRET^1$ and $BRET^2$ systems are suboptimal for small animal imaging use. To overcome their short falls, many variants of BRET systems utilizing *Renilla* luciferase mutants (RLuc8 or RLuc8.6) with mOrange ($Em_{max}$ 564 nm), TagRFP ($Em_{max}$ 584 nm), or TurboFP635 ($Em_{max}$ 635 nm) FPs were rapidly developed by us as described in the previous section (Table 10.2). All these efforts were made with the goal of finding an optimal BRET assay that is most suitable for animal imaging applications. Together, these systems also give an edge in performing multiplexed BRET assays in live environment. Many of these systems can now serve as a unified format for in vitro measurements as well as physiologically relevant BRET experiments using live cells and mice models.

To date, the advancement in the field of multiplexed approach for detecting higher-order complexes has been facilitated by creative approaches like sequential RET (SRET) [82, 83], bimolecular fluorescence complementation-BRET (BiFC-BRET) [84, 85], complemented donor–acceptor resonance energy transfer (CODA-RET) [86], and bimolecular luminescence complementation-bimolecular fluorescence complementation (BiLC-BiFC) [26, 87]. We will briefly describe the SRET development here, while others are discussed later in the chapter. In the SRET technique, three potentially interacting complex-forming proteins are each

**Table 10.2** Comprehensive chart featuring key characteristics of the BRET assays developed using *Renilla* luciferase

| Assay | Donor | Acceptor | Substrate | Important features[a] |
|---|---|---|---|---|
| BRET[1] | RLuc 480 nm (Improved version using RLuc2/RLuc8) | YFP/EYFP 535 nm | Clz/EnduRen™ | 1 Efficient BRET<br>• Spectral resolution 55 nm<br>• Small dynamic range |
| BRET[2] | RLuc 400 nm (Improved version using RLuc2/RLuc8) | GFP[2] 515 nm | Clz400/protected Clz400 | 2 Efficient BRET<br>• Spectral resolution 115 nm<br>• Very large dynamic range |
| BRET[3] | RLuc8 480 nm | mOrange 564 nm | Clz/EnduRen™ | 3 Efficient BRET<br>• Spectral resolution 85 nm<br>• Large dynamic range |
| BRET[4] | RLuc8 480 nm | TagRFP 584 nm | Clz/EnduRen™ | 4 Very efficient BRET<br>• Spectral resolution 104 nm<br>• Large dynamic range |
| BRET[5] | RLuc8 515 nm | TagRFP 584 nm | Clz-*v* | 5 Less efficient BRET<br>• Spectral resolution 70 nm<br>• Moderate dynamic range |
| BRET[6] | RLuc8.6 535 nm | TagRFP 584 nm | Clz/EnduRen™ | 6 Very efficient BRET<br>• Spectral resolution 50 nm<br>• Large dynamic range |
| BRET[7] | RLuc8 480 nm | TurboFP 635 nm | Clz-*v* | • Less efficient BRET<br>• Spectral resolution 155 nm<br>• Small dynamic range |
| BRET[8] | RLuc8.6 535 nm | TurboFP 635 nm | Clz/EnduRen™ | 7 Efficient BRET<br>• Spectral resolution 100 nm<br>• Moderate dynamic range |

[a] BRET efficiencies are categorized as less efficient, efficient, or very efficient. Dynamic ranges are categorized as small, moderate, large, or very large. Table adapted with modifications as permitted by Bentham Science [23]

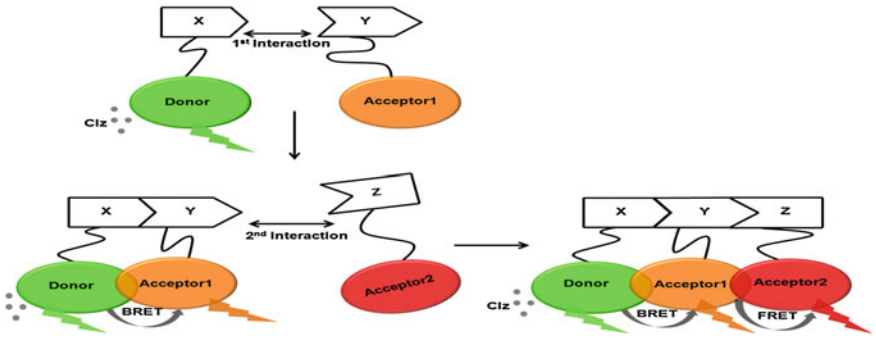


**Fig. 10.6** Schematic representations illustrating an application of sequential RET (SRET). In this scheme, three target proteins whose interaction is to be investigated are fused to either a donor or one of the two fluorescent acceptors. If donor-tagged protein X interacts with Acceptor 1-tagged protein Y, it results in a BRET process accompanied by acceptor emission upon substrate addition. If this XY dimer now interacts with a third protein Z fused to the second acceptor (Acceptor 2), a FRET process will occur between Acceptor 1 and Acceptor 2, without additional light/substrate inputs. Thus, only when all the three proteins, X, Y, and Z form a complex, both BRET and FRET signals can be seen

fused to either a donor luciferase or two acceptor FPs. Upon interaction between the donor and the first FP, the light emitted by the BRET process will fuel a FRET process between the two FPs in a sequential manner (Fig. 10.6). The development of $SRET^1$ (RLuc-YFP-DsRed) and $SRET^2$ (RLuc-$GFP^2$-YFP) utilizing Clz-*h* and Clz400 substrates, respectively, were reported in the literature for the first time. In $SRET^1$, RLuc emits at 480 nm which excites the primary BRET acceptor YFP. YFP, in turn, emits at 530 nm, which then excites a secondary acceptor DsRed through a FRET process, leading to its peak emission at ~580 nm. But, the major constraint in the utilization of $SRET^1$ system is that DsRed is tetrameric in nature, which may enhance the signal output from DsRed and can consequently give an unnaturally high SRET ratio. This downside of $SRET^1$ system can be addressed by using a monomeric red FP. On the other hand, the use of GFP and EYFP as FRET partners in the $SRET^2$ system is highly undesirable due to a low spectral resolution of only ~20 nm. Ideally, for a SRET platform to work efficiently, the three SRET partners should be so chosen, that their spectral overlap is sufficient only to ensure an optimal RET process, without having to rectify for a high signal bleed-through. Thus, this technique, though very promising, still calls for the design of more efficient SRET systems for multiplexing approaches [82].

In a broad sense, the BRET technique has so far been applied in four main areas, namely as sensors for protease, ion influx, protein–protein interactions (especially dimerization studies), and protein phosphorylation (Fig. 10.7). Taking examples from each category, we will now explain them in detail.

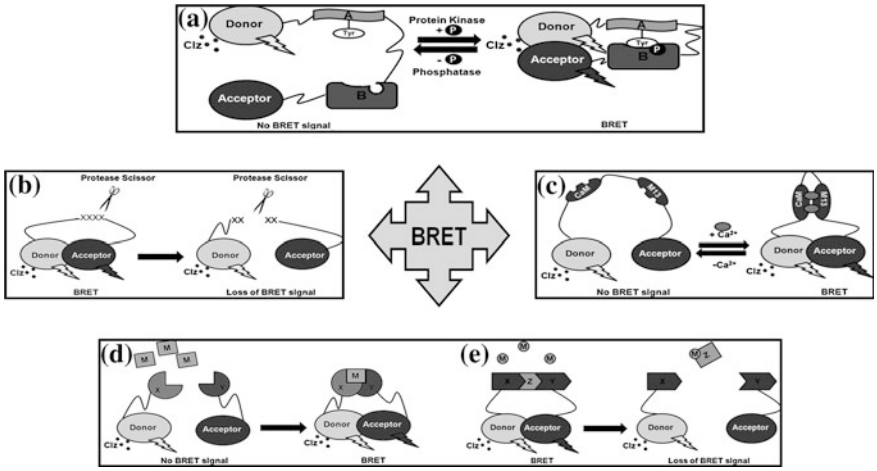


**Fig. 10.7** Schematic representations illustrating various applications of BRET. **a** BRET-based biosensor for monitoring the phosphorylation or dephosphorylation. The sensor can be designed using a substrate peptide (*A*) containing phosphorylation-specific tyrosine (*Tyr*) residue and the substrate recognition domain (*B*) such as SH2, which brings about a conformational change upon phosphorylation bringing the donor and acceptor within proximity; gain in BRET signal will be observed in case of phosphorylation or vice versa in case of dephosphorylation. **b** BRET-based probe for protease detection is shown. In this case, the protease recognition domain is situated in the linker region, and upon proteolytic cleavage, BRET signal will be lost. **c** BRET-based probe for $Ca^{2+}$ ion sensing. $Ca^{2+}$-sensing domain calmodulin (*CaM*) and M13 are present between the donor and acceptor. In calcium-deficient state, CaM-M13 complex has extended conformation (*left*). Increase in BRET signal will be seen when $Ca^{2+}$ brings CaM and M13 close to each other (*right*). **d** BRET-based sensor to monitor positive modulator (*M*) activity, which mediates the dimerization of two proteins (*X* and *Y*); BRET signal will only be observed in the presence of the modulator (*right*). **e** BRET-based senor to monitor negative modulator (*M*) activity. In the absence of modulator, a BRET signal will be observed (*left*); addition of modulator brings conformational change in the bridging protein (*Z*), disrupting the interaction of *X* and *Y,* leading to loss of BRET signal (*right*)

#### 10.4.1.1 Sensor for Protease Activity Measurement

Post-translational modification by proteolytic processing plays a crucial role in cellular functions such as peptide generation, cell cycle, and apoptosis. Such a process is also implicated in diseased conditions such as tumor metastasis, HIV, and Alzheimer's diseases. BRET can be applied to assess real-time proteolysis in living cells. In a study, a BRET-based protease sensor was developed to study peptide processing of nocistatin (NST) and nociceptin/orphanin FQ (N/OFQ) by using a novel VLuc-EYFP system [60]. As VLuc is secretory in nature, direct measurements of protease activity from the spent media make it an attractive system. To design the sensor, the NST/Noc peptide sequence was sandwiched between the VLuc-EYFP BRET probes. This peptide is bridged by a proteolytic cleavage motif of Lys-Arg. A similar RLuc-GFP BRET probe with NST/Noc propeptide was also prepared for the comparison of BRET performance. Upon

protease induction, it was found that the level of BRET activity in the spent media had decreased significantly.

To measure human immunodeficiency virus type-1 protease (HIV-1 PR) activity, a sensor was developed using $BRET^2$ system [88] by placing the HIV-1 Gag-p2/Gag-p7 protease sites in between $GFP^2$ and hRLuc. The vector comprising hRLuc-p2/p7-$GFP^2$ was coexpressed with HIV-1 codon-optimized PR + and PR- Gag/Pol expressor, resulting in a reduction or no change in $BRET^2$ signal, respectively. Such a biosensor can be adapted to high-throughput screening (HTS) assays for screening new HIV-1 protease inhibitors and/or study of viral maturation. Similarly, a $BRET^2$ biosensor for detection of feline calicivirus (FCV) was also developed [89]. By incorporating a functional or truncated FCV protease site within the $BRET^2$ biosensor, they created $BRET^2$-FCV-Cut or $BRET^2$-FCV-Uncut, respectively, and tested in feline cells. BRET assays can detect very low quantities of protease or protease inhibitor, making it ideal for an HTS platform.

Similarly, in another study, a thrombin protease target peptide was used to monitor the thrombin protease activity [90]. In this study, the RLuc molecule was inserted either at the N-terminal or C-terminal of $GFP^2$, producing RLuc-RG-$GFP^2$ and $GFP^2$-RG-RLuc fusions, respectively, where RG refers to the Arg-Gly cleavage site specific for recognition by the thrombin protease. In line with the results reported by other groups, the $GFP^2$ at the N-terminus of the fusion protein yields better signal. Further, in this study, a direct quantitative comparison was made between $BRET^1$ and $BRET^2$ systems and contrary to previous findings, $BRET^2$ appears to be a better system which can be further improvised by the use of mutant donors such as RLuc2 [24].

#### 10.4.1.2 Sensor for Ion Influx Measurement

**Calcium sensors**—$Ca^{2+}$ is a ubiquitous second messenger molecule that plays a pivotal role in important cellular and physiological functions such as neurotransmission, muscular contraction, hormone secretion, etc. Determining the dynamic changes in intracellular concentration of $Ca^{2+}$ has always been an area of exploration as even a slight disturbance in the $Ca^{2+}$ homeostasis can contribute to the manifestation of cardiac and neuronal functions. There are, however, certain limiting factors in the determination of intracellular $Ca^{2+}$ levels. For instance, the rise and fall in $Ca^{2+}$ are very fast, and that change is restricted to a narrow time frame (microseconds) and concentration (100 nm–100 mm). Aequorin [91], which functionally behaves as a luciferase, has three binding sites for $Ca^{2+}$. $Ca^{2+}$ binding stimulates a conformational change in aequorin that ultimately results in the oxidation of Clz [92] and light emission ($Em_{max}$ 470 nm). However, aequorin has a poor quantum yield; so, in such sensors, it is generally coupled to GFP or other FPs to produce chimeric proteins, wherein GFP acts as an amplifier of the photon signal from aequorin through chemiluminescence resonance energy transfer (CRET) and then emits at 510 nm. The advantage of using aequorin in the detection of $Ca^{2+}$ is that it exclusively binds to only $Ca^{2+}$. In addition, it is non-toxic, relatively

pH-insensitive [93], and does not affect the intracellular $Ca^{2+}$ concentration due to its low affinity for $Ca^{2+}$ ($K_d = 10$ μM) [92], which allows for the detection of [Ca]$^{2+}$ from $10^{-7}$ to $10^{-3}$ M. It can also be targeted to different subcellular compartments [93], such as the mitochondrial matrix. Bakayan et al. [93] fused several RFPs with aequorin, of which tdTomato was reported to be the best acceptor, owing to its high quantum output and wide absorbance spectra that has allowed $Ca^{2+}$ imaging from live animals as well. The tdTomato-Aequorin (tdTA) system could successfully image $K^+$-induced voltage-gated $Ca^{2+}$ ion channels upon membrane depolarization in primary culture of mouse neurons as a time-dependent function. In addition, the tdTA system could also monitor the intracellular $Ca^{2+}$ oscillations in cells in response to extracellular agonists.

In an alternative approach, the use of the affinity of calmodulin (CaM) for $Ca^{2+}$ has been reported. This approach is shown to be more useful over the conventional aequorin-based system when long-term imaging of $Ca^{2+}$ is required. Interaction of CaM to its target peptide M13 is mediated via the binding of $Ca^{2+}$ ion (Fig. 10.7c). This principle is made use of in a wide variety of FRET-based $Ca^{2+}$ sensors [94–96]. Saito et al. [97] developed a similar BRET-based $Ca^{2+}$ sensor using RLuc8 and different versions of Venus. The donor and the acceptor are joined to either CaM or M13. The binding of $Ca^{2+}$ to the CaM domain is reversible, and this induces a conformational change in the CaM-M13 fusion protein, making it either extended or compact, thereby changing the BRET signal. In an attempt to further optimize the BRET output, Saito et al. tried out different versions of Venus including several circularly permuted Venus (cpVenus) proteins in opposite orientations with RLuc8. In some FPs such as EGFP or ECFP, it has been observed that their fluorescence remains unaffected upon cleavage at specific points within their amino acid backbone, especially at site 144, if their C-terminal and N-terminal are linked together by a short peptide linker. Such modified FPs are called circularly permuted FPs or cpFPs and are conferred with greater sensitivity to pH and temperature. Venus-CaM-M13-RLuc8 shows the highest dynamic range (60 %), followed by RLuc8-CaM-M13-Venus, RLuc8-CaM-M13-cp157Venus, and cp229Venus-CaM-M13-RLuc8, each of which had a 30 % dynamic range. This quantitative $Ca^{2+}$ probe could successfully visualize the intracellular $Ca^{2+}$ dynamics at the single-cell level in plant and mammalian cells [97].

#### 10.4.1.3 Sensor for Protein Dimerization Measurement

One of the most straightforward applications of BRET technology has been in the study of protein dimerization particularly in the context of GPCR/receptor oligomerization studies, ligand–receptor binding studies, and drug screening assays. Exhaustive work has been done over the last decade in these areas. Covering every aspect of BRET studies in GPCRs is not the purpose of this chapter, and thus a comprehensive summary of some of the important strategies are discussed here.

To explain the concept of protein dimerization, we will be discussing the frequently used model example of rapamycin-mediated heterodimerization of FRB

and FKBP12 domains, which has been a standard proof of principle system to establish the validity of new BRET systems developed during the past decade [30, 98]. Rapamycin is a small macrolide antibiotic known for its anti-fungal and immunosuppressive activities. It targets the 12-kDa receptor immunophilin FK506-binding protein (FKBP12) in cells. Together, this rapamycin–FKBP12 complex can bind to the 11-kDa FKBP12–rapamycin-binding domain (FRB) that inhibits the kinase activity of mammalian target of rapamycin (mTOR) protein [99]. To validate a BRET system, one can design two fusion tags, the donor and acceptor, each of which is genetically fused to either FRB or FKBP12. For instance, while validating the improved $BRET^2$ using RLuc mutants or new BRET systems developed such as BRET3 to BRET6, FRB and FKBP12 model has been used to demonstrate the power of each. In all of these studies, FRB and FKBP12 are inserted in between the respective donor and acceptor pair used. Even though flexible linker amino acids were not used in the fusion protein sequence, rapamycin could induce the heterodimerization of FRB and FKBP12 and as indicated by control equivalent BRET ratio was observed. Moreover, the magnitude of the BRET signal was shown to be Rapamycin dosage dependent (Fig. 10.8). Further, in an independent experiment, it has been shown that engineered cells overexpressing the $GFP^2$-FRB-FKBP12-RLuc8 biosensor show a BRET signal gain or loss in the presence or absence of rapamycin mediator in the culture media, respectively. These studies together suggest that using this approach, HTS drug screening platforms can be designed, wherein the candidate drugs are added to live cell environment directly to measure their modulatory effects on the target protein interactions [24, 30].

As mentioned earlier, BRET-based GPCR studies were conducted to answer questions like whether a particular receptor subtype has a tendency to homodimerize or heterodimerize or both, the effect of a receptor agonist/antagonist on the dimerization state and activity of the receptor, the interaction of a receptor with other enzymes like kinases or regulators, and to understand whether the active form of a receptor is monomeric or oligomeric [34, 100–102]. In a typical GPCR study, the receptor is fused to both the donor and the acceptor at either N-terminus or C-terminus to verify the best possible orientation. The orientation that demonstrates the best BRET signal is then taken forward for the detection of the receptor oligomerization state in the presence or absence of the receptor agonist/antagonist [103]. Further advancement was exemplified by Carriba et al. who studied the heteromeric complexes of more than two neurotransmitter receptors [82]. Using SRET, they identified complexes of cannabinoid $CB_1$ receptor ($CB_1R$), dopamine $D_2$ receptor ($D_2R$), and adenosine $A_{2A}$ receptor ($A_{2A}R$) in living cells.

To study the interaction between $Ca^{2+}$-binding proteins CaM, $A_{2A,}$ and $D_2$ receptors Navarro et al. used $SRET^2$ system described before, which provides evidence for the CaM-$A_{2A}$-$D_2$ oligomerization [83]. This model has utility in basal ganglion disorder, since $A_{2A}$-$D_2R$ receptor heteromers are considered as potent target for anti-parkinson's agent. Thus, these systems were indicated for use as multi-drug screening platform.

Another approach to study the $CB_1R$, $D_2R$, and $A_{2A}R$ employs the bimolecular fluorescence complementation coupled with BRET (BiFC-BRET), which was

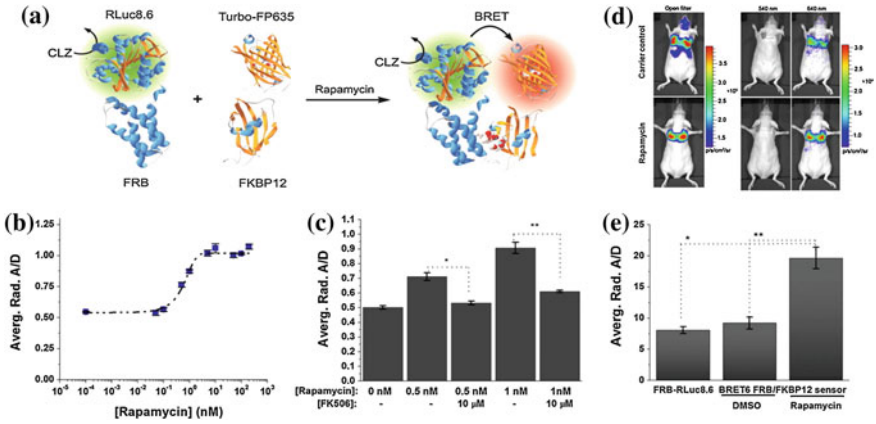


**Fig. 10.8** Characterization of the genetically encoded FRB-FKBP12 BRET6 sensor. **a** Schematic illustration of the BRET6 ($TruboFP_{635}$-RLuc8.6) sensor for monitoring the rapamycin induced FRB-FKBP12 association. **b** Rapamycin dose response curve for live HT1080 cells expressing BRET6 FRB-FKBP12 sensor. HT1080 cells ($1 \times 10^5$) expressing both FRB-RLuc8.6 and FKBP12-TurboFP635 sensor components were plated in black well plates, incubated with increasing concentrations of rapamycin and imaged spectrally using IVIS-200 at 6 h. The data were fitted to a sigmoidal curve fitting (EC50 = 0.7 ± 0.2 nm); error bars represent standard deviation. **c** Inhibition of rapamycin-induced FRB-FKBP12 association by FK506. HT1080 cells were incubated for 6 h with rapamycin (0, 0.5, and 1 nm) and with and without FK506 (10 μM), followed by imaging as described above. **d** Representative bioluminescence images of HT1080 cells stably expressing FRB-FKBP12 BRET6 sensor accumulated in the lungs of nude mice. Cells ($3 \times 10^6$ in 150 μL PBS) were injected through the tail vein, resulting in significant trapping in the lungs. One group of mice (n = 8) was injected 2 h before cell injection with 40 μg rapamycin dissolved in 20 μL DMSO and further diluted in 130 μL PBS administered through the tail vein. The control group of mice (n = 8) was injected with DMSO (20 μL in 130 μL PBS). Two hours after cells injection, the mice were injected with Clz substrate intravenously and sequentially imaged using open/donor/acceptor filters. **e** Average A/D values for BRET6 FRB-FKBP12 sensor (rapamycin and DMSO-treated groups) and donor-only FRB-RLuc8.6 calculated from mice lung-trapping model imaging experiments; error bars represent the SEM. *Note that BRET6 is now renamed as BRET8 in this chapter*. Figure represented with permission from PNAS [36]

developed by Navarro et al. [85]. In this system, they used the truncated forms of YFP fluorophore, the N-terminal truncated as Nyfp, and C-terminal truncated as cYFP. The truncated nYFP and cYFP were tagged with $CB_1R$ and $A_{2A}R$, respectively. When $CB_1RnYFP$ and $A_{2A}RcYFP$ receptors were cotransfected, the fluorescence was observed at 530 nm. No fluorescence was detected when cells were cotransfected with $A_{2A}RcYFP$ and nYFP or with $CB_1RnYFP$ and cYFP. The dopamine $D_2$ and $D_4$ receptors were tagged with RLuc to form $D_2RLuc$ and $D_4RLuc$ which serve as positive and negative controls, respectively. When $D_2RLuc$ was cotransfected with $A_2ARcYFP$ and $CB_1RnYFP$, the BRET signal was specific and was assessed by the energy transfer from donor to the complemented bimolecular fluorophore (by the interaction of $A_2ARcYFP$ and $CB_1RnYFP$). This approach has a distinct advantage over SRET. In SRET, since all the interacting partners are tagged to distinct donor or acceptors, chances of increase in

spatiotemporal change in the tagged proteins due to steric hindrance is likely. On the other hand, in BiFC-BRET, the donor is tagged to one protein, while the other two proteins are tagged to complementable fluorophores which significantly reduce the steric forces.

Urizar et al. developed the complemented donor–acceptor resonance energy transfer (CODA-RET) [86], where complementation of donor subunits tagged with dopamine $D_1$ and $D_2$ receptors constitute the luminescence signal, which further transfer resonance energy to an FP tagged with G-protein subunit. These systems have the potency to be used with agonist/antagonist-induced receptor heteromerization studies and as a tool to screen drugs and its pharmacological analysis.

Guo et al. combined luminescence and fluorescence complementation to study resonance energy transfer (BiLC-BiFC) [87]. To study the maximum receptor oligomerization with minimal tagging, split luciferase (RLuc8) was tagged to dopamine receptor $D_2$ ($D_2$-$L_1$ and $D_2$-$L_2$), and split fluorophore (mVenus) was also tagged to dopamine receptor $D_2$ ($D_2$-$V_1$ and $D_2$-$V_2$). The tetramerization of $D_2$-$L_1$-$D_2$-$L_2$-$D_2$-$V_1$-$D_2$-$V_2$ was studied. A major bottleneck in the utilization of any of the above-mentioned complementation approaches is the severe loss of signal when split luciferases or split fluorophores are used. With suitable engineering to improve the split reporter performance and the use of more sensitive detection instruments, this approach might be feasible in the future.

#### 10.4.1.4 Sensor for Phosphorylation Measurement

Protein phosphorylation is an important post-translational modification that controls many aspects of cellular signaling in multicellular organisms. Protein kinases phosphorylate the protein at specific serine, threonine, or tyrosine residues by the addition of covalently bound phosphate group. Upon phosphorylation, substrate proteins are subjected to conformational changes due to the negative charge of the phosphate groups, which subsequently triggers their enzymatic activation and interaction with target proteins. Ideally, interactions of phosphorylated proteins should be studied in the physiological context and in real-time, and thus, a BRET-based method provides an advantage. To study protein phosphorylation using BRET technology, two basic types of phosphorylation sensors can be designed. In the first approach, a tandem fusion of substrate domain and phosphorylation recognition domain is sandwiched between donor–acceptor pair (Fig. 10.7a). In the second approach, a sensor to study the formation of homo- or heterodimers of receptor tyrosine kinases [104, 105] or its downstream effector proteins [106] can be designed.

The Src homology 2 (SH2) domain is the most prevalent of substrate recognition modules and plays a central role in tyrosine kinase signaling pathways. The human genome contains a total of 120 such SH2 domains in 110 distinct proteins. SH2 domain is relatively small ($\sim$100 amino acids) and can fold independently; hence, the isolated domain can be expressed independently and used for direct binding assays. The SH2 domains also differ in their binding preferences for specific phosphorylated ligands, resulting in specificity in signal transduction.

Using such strategy, though FRET-based direct phosphorylation sensing was demonstrated [107], BRET applications are yet to come. The only BRET-based study that demonstrated the existence of the preassociated STAT3 molecules in the cytoplasm of live cells as dimers or multimers is by Schröder et al. They questioned the belief of activation-induced STAT3 dimerization in cytoplasm and provided an alternative hypothesis [108]. Thus, the reconsideration of STAT3 activation pathway was addressed using BRET[1].

#### 10.4.1.5 Miscellaneous Sensors

While most of the work done using BRET technology represents the categories mentioned above, there are some very unique BRET sensors developed that are worth mentioning and have raised the applicability of BRET to the next level. Arai et al. [109] designed an immunoassay platform that can detect the presence of an antigen in a solution using BRET. Coined as open sandwich bioluminescent immunoassay (OS-BLIA), this assay comprises of the variable heavy and light chains of an antibody against the hen egg lysozyme fused to the donor (RLuc) and acceptor (EYFP) proteins, respectively. The only prerequisite for the assay to work is that the antibody variable region should have a negligibly weak $V_H$-$V_L$ interaction in the absence of its antigen followed by the formation of a stabilized association upon the addition of the bridging antigen. The $V_H$ and $V_L$ proteins are both conjugated to thioredoxin (Trx) which has been shown to enhance the binding efficiency of these proteins to the antigen [109]. This sensor showed an antigen-dependent increase in BRET signal output, with signal saturation at an antigen concentration above 100 μg/mL. Although the dynamic range of this assay is miniscule ($\sim$0.14 only), this assay is one of its kind and opens up a new avenue in BRET-based assays. Moreover, its requirement for only a single antibody provides a definite advantage and obviates the need for a second antibody (against another epitope on the antigen) as in the case of sandwich ELISA. With further optimization, this assay might prove promising as antigen detection kits.

Another novel application of BRET technology is in the detection of specific RNA sequences that may again be used to develop RNA detection kits. In this area, two different studies have successfully designed suitable BRET-based assay. The first technique was pioneered by Walls et al. [110], which comprised of a dual probe system. The first probe consisted of a 20-mer oligonucleotide complementary to a specific RNA sequence (in this case the FLuc cDNA/mRNA) and conjugated at its 5′ terminal to RLuc8. The second probe consisted of another 20-mer oligonucleotide (which is again complementary to the same target RNA but at a different locus than the previous one) and conjugated at its 3′ terminal to GFP[2]. The biotinylated target mRNA which is immobilized on a streptavidin-coated 96-well black plate acts as a "scaffold" on which the two probes can bind. The successful hybridization of the probes with the target RNA brings the BRET partners in close proximity to each other, consequently leading to a positive BRET signal upon substrate addition. The BRET signal was optimal when the binding sites of the two

probes were 10 nucleotides apart (lesser distance increased steric hindrance, while greater distance reduced RET efficiency). The attractive features of this technique are its high specificity upon the use of two probes, rapid results, and the ease with which this system can be customized for every new target mRNA without affecting its efficiency. However, obstacles like low sensitivity (can detect only up to 1 μg, while RT-PCR can detect as low as 100 ng RNA) need to be minimized before its commercial diagnostic application.

Recently, Andou et al. [111] reported another RNA detection system that made use of the arginine-rich motifs (ARM) derived from RNA-viruses and flanked by hRLuc and EYFP on its either side. The ARM peptide can recognize and bind to specific RNA sequences upon which, it undergoes a conformational change which is reflected as a change in the BRET signal. Additionally, different flexible [$(GGGS)_5$] and rigid linkers [$(EAAAK)_4$ or $(EAAAK)_5$] of varying lengths were also added adjacent to the ARM peptide to monitor their effect on the BRET signal. Of the three viral ARM peptides used, namely Human Immunodeficiency Virus Rev peptide (Rev), Bovine Immunodeficiency Virus (BIV Tat), and Jembrana Deficiency Virus Tat peptide (JDV Tat), BIV Tat peptide and modified JDV Tat peptide, which are both specific for TAR RNA, adopt a $\beta$-hairpin conformation upon successful binding to the TAR RNA and show the maximum change in BRET signal, thus establishing the validity of this assay design. However, this is just a prototype and developing a uniform diagnostic platform based on this model for a diverse range of target RNAs has a long way to go.

## *10.4.2 Synthetic BRET Probes*

Recently, some high-throughput BRET systems were developed that harness the power of synthetic chemistry. As near-infrared (NIR)-emitting FPs are rare or the ones available and generally suffer from either poor stability, low excitation coefficient, or low quantum output, which are important determinants for an acceptor molecule, they have a limited use in BRET assay system development. In complementation to genetic BRET reporter systems, synthetic BRET probes viz., quantum dots (QDs) and fluorescent dyes have surfaced to overcome the limitations of genetic BRET systems.

### 10.4.2.1 BRET Using Quantum Dots

A remarkable development of QD as BRET probes has provided a new tool for resonance energy transfer systems [112]. QDs are colloidal nanocrystalline semiconductors possessing unique properties such as large stoke shift, broad excitation and narrow size-tunable emission spectra, negligible photobleaching, and high photochemical stability, which make them highly suitable fluorophores for use as a BRET acceptor (Fig. 10.9). The surface of QDs has a crucial effect on

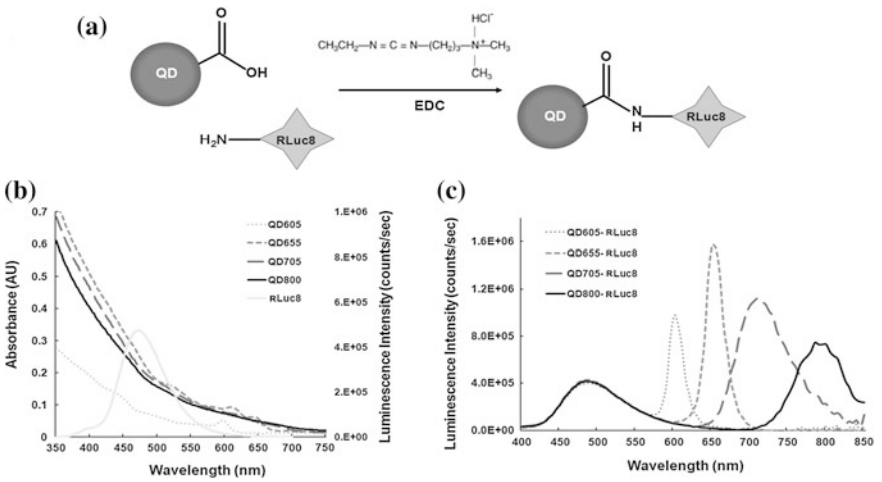


**Fig. 10.9** Schematic illustration of QD BRET assay system. **a** QDs are linked to a bioluminescent *Renilla* luciferase mutant protein (RLuc8) by chemical bonding. It is possible to link up to six RLuc8 protein molecules on each QD surface and insert various linker sequences (such as protease recognition sequence) to develop biosensor probe. **b** Chart showing absorbance curves of selected color variant QDs which basically vary by their sizes. The chart is superimposed with RLuc8 luminescence emission curve (luminescence scale bar on *z*-axis), indicating that RLuc8 protein can be used as donor for all the size variant QD's to obtain BRET-based QD emission. **c** Chart showing luminescence intensity versus wavelength curves captured by exposing the color variant QD-RLuc8 molecules to coelenterazine substrate, providing multiplexing opportunity for spectral imaging. Figure adapted with modifications as permitted by NPG [112]

photoluminescence. This can be understood by the concept of trap states, which are caused by structural defects, such as atomic vacancies, local lattice mismatches, dangling bonds, or adsorbates at the surface. Excited electrons or holes can be trapped by these trap states, leading to non-radiative recombination. Surface passivation by overcoating the QDs with CdSe coated with ZnS (such semiconductors provide a wider band gap) can be used to minimize this trapping. This increases the photostability of the core, and hence, the quantum yield, making these core–shell-structured QDs more favorable for fluorescence-based applications [113].

A pioneering study reporting the development of QD-BRET system comprises the *Renilla* luciferase mutant (RLuc8) conjugated to the polymer-coated CdSe/ZnS core–shell QD655 ($Em_{max}$ 655 nm) through coupling of amino groups on RLuc8 to the carboxylated group presented on QDs [112]. Gel electrophoresis can confirm the conjugation of QD655-RLuc8. The hydrodynamic diameter of QD655-RLuc8 was estimated to be $\sim$2 nm larger than that of QD655. Each QD655-RLuc8 conjugate was estimated to contain on an average six RLuc8 molecules as donor. On addition of Clz to QD655-RLuc8, in addition to the Rluc8 emission at 480 nm, a strong peak at 655 nm was detected, indicating non-radiative energy transfer to the QD655. By applying synthetic chemistry, distance-dependent variation in the BRET ratio was tested. Further, the QD655-RLuc8 BRET probe stability has been

tested in vitro in mouse serum. The multiplexing approach has also been demonstrated, utilizing QD605, QD655, QD705, and QD800 tagging with the same RLuc8 protein yielding BRET ratios of 0.70, 1.20, 2.30, and 1.32, respectively. The spectrally distinct emission of these four conjugates can enable multiplexed BLI. Such multiplexing opportunities are unique amongst all the BRET probes designed so far, which provides an option for the user to choose the size of QD based on their intended use in cell-based or animal imaging.

Since the conjugation of QD and luciferase is random, the orientation of both the moieties can influence the sensitivity of the BRET protease assay. An intein-mediated chemical method can be recruited which specifically controls their relative orientation as well as restrict the number of conjugated RLuc8 moieties to one. Intein is a polypeptide sequence inside a protein that is able to excise itself and rejoins the remaining portion with a peptide bond. Further, QD-BRET systems were adopted to detect the cellular protease activity. A series of QD-BRET biosensors were synthesized for detection of MMP-2, MMP-7, and urokinase-type plasminogen activator (uPA) activity. These sensors having varied sensitivity can easily detect protease in serum [114]. QD655-MMP7-RLuc8 BRET was assayed with increasing amount of MMP-7 protease. Since the protease specifically cleaves off the peptide between the QD655 and RLuc8, the signal at 575–650 nm emission filter decreases and so will the BRET ratio. A similar decrease in BRET signal was observed for QD655-MMP2-RLuc8 and QD655-uPA-RLuc8 sensor when incubated with the MMP-2 and uPA proteases in buffer and serum. Simultaneous detection of MMP-2 and uPA proteases by spectrally resolved QD655-MMP-2-RLuc8 and QD705-uPA-RLuc8 was performed. The multiplexing ability of varied QD-BRET systems can provide a useful tool for the detection of many proteases/targets in a sample. A QD-BRET approach has also been demonstrated for nucleic acid detection [115].

#### 10.4.2.2 BRET Using Fluorescent Dyes

As the use of QD-BRET is limited due to bulky size and toxicity of QD itself, fluorescent dyes having low molecular weight, extended absorption spectra, high stability, and high photon output may offer advantages as synthetic BRET probes. In a recent literature, conjugation of the luciferase protein CLuc (*Cypridina* luciferase) with a far-red fluorescent dye Indocyadine via a glycol chain was reported to form a far-red bioluminescent protein "FBP" [116]. CLuc oxidizes *Cypridina* luciferin to yield a light emission peak at 460 nm. A biotinylated FBP was tagged with a monoclonal antibody against human delta-like protein-1(Dlk-1) using a biotin–avidin interaction. This probe was used in the BLI of cancer cells in vitro and in vivo. The use of a self-illuminating probe eliminates the need of external illumination; rather, it is readily detectable upon substrate addition.

As reported in literatures, modification at cysteine and lysine residues of luciferase by chemical methods severely impairs their bioluminescence activity.

Branchini et al. [117] reported a firefly luciferase variant having point mutations to incorporate two cysteine residues, which permits the binding of dyes to the luciferase without destroying the native cysteine residues and preserving the bioluminescence activity of luciferase. BRET-based probes emitting in NIR region were developed by coupling an FLuc mutant (as donor; $Em_{max}$ 617 nm) to Alexa Fluor® 680 ($Em_{max}$ 705 nm) or Alexa Fluor® 750 ($Em_{max}$ 750 nm) as acceptor. Branchini et al. [52] further reported the design of a single soluble probe based on the SRET principle. This probe comprises of a thermostable firefly luciferase ($Em_{max}$ 560 nm) linked via different proteolytic target peptide sites to an mKate variant ($Em_{max}$ 620 nm) covalently labeled with two Alexa Fluor® 680 ($Em_{max}$ 705 nm). These probes enable the detection of protease activity in NIR, making it an attractive system for animal imaging.

#### 10.4.2.3 BRET Using Carbon-60

Utilizing the luminescence quenching and free radicals scavenging properties of carbon-60 fullerene ($C_{60}$) derivatives, a novel BRET system was constructed for protease detection in combination with hGLuc [118]. The free radical quenching property of $C_{60}$ is attributed to the delocalized $\pi$ bond, curvature of its surface, and electron deficiency. Here, two different fullerene derivatives, carboxyl $C_{60}$ ($C_{60}[C(COOH)_2]_3$) and amino hydroxyl $C_{60}$ ($C_{60}(NH_2)x(OH)y$), have been examined to see whether they have any special effects on hGLuc luminescence. The strong absorption of $C_{60}$–COOH in the wavelength range of 425 nm to 525 nm indicates that $C_{60}$–COOH could be a good quencher not only for hGLuc but also for other luciferases, therefore providing a good acceptor in BRET assays. This assay works on the principle of attenuation of bioluminescence from hGluc by $C_{60}$. As the peptide joining hGLuc and $C_{60}$ is severed off, gain in bioluminescence signal is detected. The high sensitivity obtained for detection of a thrombin protease demonstrated that $C_{60}$–COOH– $(Ni)^{+2}$–hGLuc system is an efficient system and can facilitate the testing of longer peptide linkers for many other protease assays in the future.

## 10.5 Engineering BRET Measurement Equipments

### *10.5.1 Microplate Reader*

Since its inception in biological research, BRET signal is quantitatively measured using photomultiplier tube (PMT)-based microplate reader equipments. Scanning spectroscopy or a suitable plate reader capable of sequential or simultaneous detection of the two distinct wavelength ranges can be quantified for determining BRET efficiencies. Microplate measurements of BRET signal has so far been limited by its association with substrate injection before signal measurement from

each well of a multi-well plate. As discussed in the previous section, an important landmark development in live cell BRET measurement was achieved by the introduction of live cell substrate e.g., EnduRen™ which greatly stabilizes the RLuc flash kinetics. Availability of live cell Clz-*h* or Clz400 substrates would definitely help further automation toward developing a high-throughput screening methodology using BRET. In the following sections, we will address the issue of validating the BRET assay to compensate for the false-positive results.

While counting photons using plate reader in BRET PPIs studies, especially for the receptor oligomerization studies, there is a very high probability of artifacts if the concentration of the expressed receptor is high. In such a situation, the increased abundance of receptors means that there is a greater chance of two receptors being within the BRET-permissive distance of each other, leading to random collisions and consequently non-specific BRET, a phenomenon known as bystander BRET [101]. To distinguish between the genuine and random BRET interactions, appropriate controls must be recruited. As an appropriate negative control in the BRET assay, the acceptor FP without fusing it to another protein can be used. Alternatively, when receptors are being studied, one can also make use of a protein that is expressed at a similar level to the target receptor, but which does not interact with the other target protein [27]. A suitable positive control to use in conjunction with the BRET assay is the donor and acceptor molecules fused to each other through a flexible linker [27]. This can give us an indication of the highest possible BRET signal that can be achieved for a particular BRET pair.

#### 10.5.1.1 BRET Dilution Assay

In this assay, the concentrations of both the donor and the acceptor fusion proteins are gradually diluted till the bystander BRET can be sufficiently eliminated. Theoretically, the BRET signal can be denoted by Eq. 10.5.

$$\mathrm{BRET} = \mathrm{BRET}_0 + k([D] = [A]) \tag{10.5}$$

where $[D]$ and $[A]$ are donor and acceptor concentrations, respectively. By simultaneously lowering the concentration of both receptors (dilution) at a constant $[A]/[D]$ ratio, the BRET signal decreases toward $\mathrm{BRET}_0$, which is the real oligomerization signal. This assay can then be used to set the optimal donor and acceptor concentrations for BRET saturation assays [26].

#### 10.5.1.2 BRET Saturation Assay

This assay involves coexpressing a constant amount of donor fusion protein with a gradually increasing concentration of acceptor-tagged protein. The concentration of the donor protein is determined to be the minimum concentration of donor which gives a reliable and detectable signal output (as previously determined by the dilution

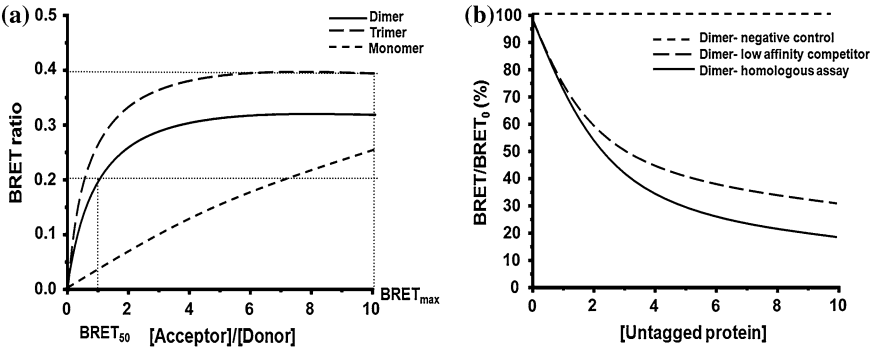


**Fig. 10.10** Chart illustrating various assay parameters that validate the BRET assay. **a** The expected BRET saturation curves obtained as a function of the ratio of concentration of acceptor- and donor-tagged receptor molecules. The sigmoidal curve represents a true BRET event, while a linear plot is seen due to bystander BRET. The saturation in BRET signal is denoted by $BRET_{max}$ which is the highest possible BRET activity. Note that receptor trimerization can achieve a faster saturation compared to dimmers, as can be seen by a lower $BRET_{50}$ value which is the [A]/[D] ratio required to obtain a 50 % $BRET_{max}$. **b** Hypothetical BRET competition assay as a function of the untagged competitor molecule concentration. As the concentration of untagged receptor increases, it will compete with the tagged receptors to form dimers. In the negative control, a non-competing protein is used, where the BRET activity of the target receptors remains unaffected. In the homologous assay, the same kind of receptor as the target receptor is taken as the competitor that will maximally affect the receptor oligomerization of the BRET partners; while in the other case, a different receptor type with lowered binding affinity to the receptors is used as the competitor

assay). In this case, the BRET signal will increase till all acceptor molecules are interacting with the available donor molecules and a $BRET_{max}$ signal is achieved. Beyond this, an increase in acceptor concentration will not affect the BRET signal [26]. The higher the oligomerization state of the receptor, the faster the saturation can be achieved (Fig. 10.10a). Thus, if the experimental data can be fitted to match these theoretical curves, it reflects the specificity of receptor interactions [103]. Moreover, by comparing the $BRET_{50}$ values (the receptor concentration at which the BRET signal is 50 % of its maximum value) for homodimers and heterodimers, a saturation assay can help evaluate the relative affinity for their formation.

### 10.5.1.3 BRET Competition Assay

In this assay, the donor- and acceptor-tagged proteins are coexpressed with constant or increasing concentrations of untagged proteins which will compete with the tagged proteins for binding with the other tagged proteins. The decrease in the BRET output due to competitive inhibition provides evidence for the specificity of protein–protein interactions (Fig. 10.10b).

### 10.5.2 BRET Imaging Microscope

The ability to identify the subcellular location of interacting proteins and quantitative assessment of the changes undergoing therein provide a clear advantage over spectrophotometric BRET analysis from cell populations using a microplate reader. Bioluminescence microscopy (BLM), as its name suggests, uses luminescence rather than fluorescence. Like fluorescence imaging, BLM enables the visualization of genetic expression and physiological processes at the molecular level in living tissues. Imaging cells by exploiting luminescence reaction has several advantages over fluorescence. First, repeated exposure of living cells or tissues to fluorescence excitation wavelengths can photodamage the cells or photobleach the fluorophore, while bioluminescence is not burdened by such phototoxic or photobleaching effects. Also, unlike fluorescence, bioluminescence imaging typically does not suffer from auto-fluorescence background signal. The resulting high signal-to-background ratio allows more straightforward signal quantification and more sensitive signal detection. Furthermore, only viable cells emit luminescence signals, and thus measurements are absolute and directly quantitative, making live cell imaging much more suitable for long-term imaging. However, despite these advantages, applications for luminescence in live cell imaging have been limited until now, primarily due to the lack of sensitive detection device which can resolve low photon emission from micron-size space. Because luminescence is much dimmer than fluorescence, it requires longer capture time. Though the optics components required for luminescence detection are simpler, the availability and cost of the detection devices like intensely cooled charge-coupled device (CCD) cameras were the main constraint until a few years back. Furthermore, it is difficult to resolve spatial information with the subcellular, ultra-structural details as is possible with fluorescence microscopy today. Therefore, most systems in use have been built specifically by the researchers using components that are best suitable for their experimental requirements [106]. For instance, Xu et al. [119] used a microscope equipped with a modified electron bombarded charge-coupled device (EB-CCD) camera and a dual-view microimager attached directly to a 4x microscopic objective. Later on, Coulon et al. [120] demonstrated subcellular measurement of BRET signal using a modified version of inverted microscope equipped with electron-multiplying cooled charge-coupled device (EMCCD) camera. Recently, we have also demonstrated live cell imaging using BRET3 assay and a commercial luminescence microscope [30].

### 10.5.3 Macroscopic BRET Imaging

The ability to non-invasively image PPIs from their natural physiological environments has an important implication on a wide variety of biological research endeavors, such as drug discovery, molecular medicine, etc. With the introduction

of the intensely cooled CCD camera-based optical imaging instrumentation, the ability to detect very dim photon signals from live cells in culture or from animal or plant tissues has become possible. To detect signals with detectors placed outside the animal subjects, the cells of interest present at a depth within the subject must produce detectable signal. Here, the use of red and NIR light signals is favored as they have better tissue penetration capacity. Therefore, overall modification of existing assays to adapt them for non-invasive monitoring is a challenging task. Approaching the development of a single-format imaging assay that can serve to measure PPIs from isolated single cells as well as physiologically relevant animal/plant models, both $BRET^1$ and $BRET^2$ strategies, display some form of confinements. Therefore, while attempting live animal BRET assays, we have conducted serial experiments to identify an optimal BRET assay showing satisfactory performance as a single-format assay [24, 30, 98]. By now, we have ample variety of the red-light-emitting BRET vectors (as mentioned in Table 10.2) developed, many of which undoubtedly show superior performance over the previous assays used. By withdrawing the traditional method of BRET measurement using a microplate reader, we adapted a method for spectral separation of donor and acceptor signal by using a black-box cooled CCD camera macroimager [98]. An important parameter to successfully adapt this imaging method was the use of the BRET formats with relatively large spectral resolution, which allows the selection of wide band-pass emission filters in the device. Unlike the plate reader, the CCD camera-based macroimaging instrument can measure BRET signals from lysed or live cells placed in multi-well plates. The same instrument can then be used for BRET measurement from whole organisms as well. Point worth noting here is that BRET imaging from animal tissue is further complicated by the consideration of tissue attenuation factor. To address this, a double ratio (DR) which provides a depth-independent measure of the BRET signal in animal experiment was defined [36].

The main bottleneck of extending FRET strategy in small animal evaluation is associated with the auto-fluorescence correction method. As light travels in and out from animal tissues, the resulting photon attenuation complicates the FRET ratio calculations. In this context, the exclusion of an external photon input makes BRET-based technologies more acquiescent for macroscale imaging. We have also done proof of principle studies by confirming the detection of the rapamycin-dependent interaction of FKBP12 and FRB from living animals [24, 30, 36] (Fig. 10.8). Following the successful BRET imaging from small animal model, macroimaging of plant tissue was also reported [119]. Visualization of the COP1 (a plant light signaling regulator protein) homodimerization using RLuc-EYFP BRET assay was demonstrated in the rootlet and cotyledons of tobacco seedlings. Considering careful validation of the PPIs in systematic, large-scale models using individual test cases, the molecular imaging assays like BRET appear promising in the current proteomic developments.

## 10.6 Future Prospects and Concluding Remarks

Tremendous developments in the field of protein interaction analysis have been fueled by current efforts in the life sciences to dissect cellular protein function. A full understanding of how the proteins function and contribute to the signaling networks in the cell requires approaches to study protein interactions from different perspectives. Once the specific and relevant interactions have been identified, in-depth characterization of the molecular and biophysical parameters such as the kinetic rate constants, the oligomeric state of the interaction partners, and the stoichiometric ratio in the complex will follow. For this part of subjective analysis of a known pair of interactors, purified and well-characterized proteins are required. However, when one has to identify the protein interaction partners and gather a detailed understanding of protein interactions at the molecular and cellular context, screening techniques that can operate in live cell environment are required. Therefore, for a thorough understanding of PPIs in normal and diseased biology, need of technologies that offer options for both in vitro as well as in vivo assessment will speed up this epic task. With the huge expansion and adjustment made as described in this chapter, bioengineered BRET systems will continue to expand and fuel this area in future. The ability to tag endogenous proteins of interest with donor and acceptor molecule within live cell environment is a challenging task, and perhaps technology will develop in future to enhance our ability to achieve that as well.

**Acknowledgments** Funding support to AD from DBT Bioengineering, New Delhi and ACT-REC, TMC, India is gratefully acknowledged.

## References

1. Selbach M, Mann M (2006) Protein interaction screening by quantitative immunoprecipitation combined with knockdown (QUICK). Nat Methods 3(12):981–983. doi:10.1038/nmeth972
2. Williams NE (2000) Immunoprecipitation procedures. Methods Cell Biol 62:449–453. doi:10.1016%2FS0091-679X%2808%2961549-6
3. Phizicky EM, Fields S (1995) Protein-protein interactions: methods for detection and analysis. Microbiol Rev 59(1):94–123
4. Rediger A, Tarnow P, Bickenbach A, Schaefer M, Krude H, Gruters A, Biebermann H (2009) Heterodimerization of hypothalamic G-protein-coupled receptors involved in weight regulation. Obes Facts 2(2):80–86. doi:10.1159/000209862
5. Ciruela F (2008) Fluorescence-based methods in the study of protein–protein interactions in living cells. Curr Opin Biotechnol 19(4):338–343. doi:10.1016/j.copbio.2008.06.003
6. Ciruela F, Vilardaga JP, Fernandez-Duenas V (2010) Lighting up multiprotein complexes: lessons from GPCR oligomerization. Trends Biotechnol 28(8):407–415. doi:10.1016/j.tibtech.2010.05.002
7. Fields S, Song O (1989) A novel genetic system to detect protein–protein interactions. Nature 340(6230):245–246. doi:10.1038/340245a0

8. Ray P, Pimenta H, Paulmurugan R, Berger F, Phelps ME, Iyer M, Gambhir SS (2002) Noninvasive quantitative imaging of protein–protein interactions in living subjects. Proc Natl Acad Sci USA 99(5):3105–3110. doi:10.1073/pnas.052710999
9. Mohler WA, Blau HM (1996) Gene expression and cell fusion analyzed by lacZ complementation in mammalian cells. Proc Natl Acad Sci USA 93(22):12423–12427
10. Piehler J (2005) New methodologies for measuring protein interactions in vivo and in vitro. Curr Opin Struct Biol 15(1):4–14. doi:10.1016/j.sbi.2005.01.008
11. Widder EA (2010) Bioluminescence in the ocean: origins of biological, chemical, and ecological diversity. Science 328(5979):704–708. doi:10.1126/science.1174269
12. Seliger HH, Mc EW (1960) Spectral emission and quantum yield of firefly bioluminescence. Arch Biochem Biophys 88:136–141
13. Koo JA, Schmidt SP, Schuster GB (1978) Bioluminescence of the firefly: key steps in the formation of the electronically excited state for model systems. Proc Natl Acad Sci USA 75(1):30–33
14. Hoshino H (2009) Current advanced bioluminescence technology in drug discovery. Expert Opin Drug Discov 4(4):373–389. doi:10.1517/17460440902804372
15. Ohmiya Y (2005) Basic and applied aspects of color tuning of bioluminescence systems. Jpn J Appl Phys 44 (9A):6368–6379. doi:10.1143/jjap.44.6368
16. Beutler E, Baluda MC (1964) Simplified determination of blood adenosine triphosphate using the firefly system. Blood 23:688–698
17. Shimomura O, Johnson FH (1978) Peroxidized coelenterazine, the active group in the photoprotein aequorin. Proc Natl Acad Sci USA 75(6):2611–2615
18. van Roessel P, Brand AH (2002) Imaging into the future: visualizing gene expression and protein interactions with fluorescent proteins. Nat Cell Biol 4(1):E15–E20. doi:10.1038/ncb0102-e15
19. Forster T (1948) Zwischenmolekulare Energiewanderung und Fluoreszenz. Ann Phys 2:54–75
20. Clegg RM (1992) Fluorescence resonance energy transfer and nucleic acids. Methods Enzymol 211:353–388
21. Wu P, Brand L (1994) Resonance energy transfer: methods and applications. Anal Biochem 218(1):1–13
22. Stryer L, Haugland RP (1967) Energy transfer: a spectroscopic ruler. Proc Natl Acad Sci USA 58(2):719–726
23. De A (2011) The new era of bioluminescence resonance energy transfer technology. Curr Pharm Biotechnol 12(4):558–568
24. De A, Loening AM, Gambhir SS (2007) An improved bioluminescence resonance energy transfer strategy for imaging intracellular events in single cells and living subjects. Cancer Res 67(15):7175–7183. doi:10.1158/0008-5472.CAN-06-4623
25. Xu Y, Piston DW, Johnson CH (1999) A bioluminescence resonance energy transfer (BRET) system: application to interacting circadian clock proteins. Proc Natl Acad Sci USA 96(1):151–156
26. Drinovec L, Kubale V, Nohr Larsen J, Vrecl M (2012) Mathematical models for quantitative assessment of bioluminescence resonance energy transfer: application to seven transmembrane receptors oligomerization. Front Endocrinol 3:104. doi:10.3389/fendo.2012.00104
27. Pfleger KD, Eidne KA (2006) Illuminating insights into protein–protein interactions using bioluminescence resonance energy transfer (BRET). Nat Methods 3(3):165–174. doi:10.1038%2Fnmeth841
28. Bacart J, Corbel C, Jockers R, Bach S, Couturier C (2008) The BRET technology and its application to screening assays. Biotechnol J 3(3):311–324. doi:10.1002/biot.200700222
29. Hamdan FF, Percherancier Y, Breton B, Bouvier M (2006) Monitoring protein–protein interactions in living cells by bioluminescence resonance energy transfer (BRET). In: Curr Protoc Neurosci. 2008/04/23 edn. Wiley, pp 5.23.21-25.23.20. doi:10.1002/0471142301.ns0523s34

30. De A, Ray P, Loening AM, Gambhir SS (2009) BRET3: a red-shifted bioluminescence resonance energy transfer (BRET)-based integrated platform for imaging protein–protein interactions from single live cells and living animals. FASEB J 23(8):2702–2709. doi:10.1096/fj.08-118919
31. Dionne P, Mireille C, Labonte A, Carter-Allen K, Houle B, Joly E, Taylor SC, Menard L (2002) BRET2: efficient energy transfer from Renilla Luciferase to GFP2 to measure protein–protein interactions and intracellular signaling events in live cells. In: van Dyke K, van Dyke C, Woodfork K (eds) Luminescence biotechnology: instruments and applications. CRC Press, pp 539–555
32. Bertrand L, Parent S, Caron M, Legault M, Joly E, Angers S, Bouvier M, Brown M, Houle B, Menard L (2002) The BRET2/arrestin assay in stable recombinant cells: a platform to screen for compounds that interact with G protein-coupled receptors (GPCRS). J Recept Signal Transduct Res 22(1–4):533–541. doi:10.1081/RRS-120014619
33. Eidne KA, Kroeger KM, Hanyaloglu AC (2002) Applications of novel resonance energy transfer techniques to study dynamic hormone receptor interactions in living cells. Trends Endocrinol Metab 13(10):415–421
34. Angers S, Salahpour A, Joly E, Hilairet S, Chelsky D, Dennis M, Bouvier M (2000) Detection of beta 2-adrenergic receptor dimerization in living cells using bioluminescence resonance energy transfer (BRET). Proc Natl Acad Sci USA 97(7):3684–3689. doi:10.1073/pnas.060590697
35. Loening AM, Fenn TD, Wu AM, Gambhir SS (2006) Consensus guided mutagenesis of Renilla luciferase yields enhanced stability and light output. Protein Eng Des Sel 19(9):391–400. doi:10.1093/protein/gzl023
36. Dragulescu-Andrasi A, Chan CT, De A, Massoud TF, Gambhir SS (2011) Bioluminescence resonance energy transfer (BRET) imaging of protein–protein interactions within deep tissues of living subjects. Proc Natl Acad Sci USA 108(29):12060–12065. doi:10.1073/pnas.1100923108
37. Caysa H, Jacob R, Muther N, Branchini B, Messerle M, Soling A (2009) A red-shifted codon-optimized firefly luciferase is a sensitive reporter for bioluminescence imaging. Photochem Photobiol Sci 8(1):52–56. doi:10.1039/b814566k
38. Loening AM, Wu AM, Gambhir SS (2007) Red-shifted Renilla reniformis luciferase variants for imaging in living subjects. Nat Methods 4(8):641–643. doi:10.1038/nmeth1070
39. Loening AM, Dragulescu-Andrasi A, Gambhir SS (2010) A red-shifted Renilla luciferase for transient reporter-gene expression. Nat Methods 7(1):5–6. doi:10.1038/nmeth0110-05
40. Fan F, Wood KV (2007) Bioluminescent assays for high-throughput screening. Assay Drug Dev Technol 5(1):127–136. doi:10.1089/adt.2006.053
41. Hall MP, Unch J, Binkowski BF, Valley MP, Butler BL, Wood MG, Otto P, Zimmerman K, Vidugiris G, Machleidt T, Robers MB, Benink HA, Eggers CT, Slater MR, Meisenheimer PL, Klaubert DH, Fan F, Encell LP, Wood KV (2012) Engineered luciferase reporter from a deep sea shrimp utilizing a novel imidazopyrazinone substrate. ACS Chem Biol 7(11):1848–1857. doi:10.1021/cb3002478
42. Stepanyuk GA, Unch J, Malikova NP, Markova SV, Lee J, Vysotski ES (2010) Coelenterazine-v ligated to $Ca^{2+}$-triggered coelenterazine-binding protein is a stable and efficient substrate of the red-shifted mutant of Renilla muelleri luciferase. Anal Bioanal Chem 398(4):1809–1817. doi:10.1007/s00216-010-4106-9
43. Giuliani G, Molinari P, Ferretti G, Cappelli A, Anzini M, Vomero S, Costa T (2012) New red-shifted coelenterazine analogues with an extended electronic conjugation. Tetrahedron Lett 53(38):5114–5118. doi:10.1016/j.tetlet.2012.07.041
44. Levi J, De A, Cheng Z, Gambhir SS (2007) Bisdeoxycoelenterazine derivatives for improvement of bioluminescence resonance energy transfer assays. J Am Chem Soc 129(39):11900–11901. doi:10.1021/ja073936h
45. Otto-Duessel M, Khankaldyyan V, Gonzalez-Gomez I, Jensen MC, Laug WE, Rosol M (2006) In vivo testing of Renilla luciferase substrate analogs in an orthotopic murine model of human glioblastoma. Mol Imaging 5(2):57–64. doi:10.2310/7290.2006.00006

46. Pfleger KD, Dromey JR, Dalrymple MB, Lim EM, Thomas WG, Eidne KA (2006) Extended bioluminescence resonance energy transfer (eBRET) for monitoring prolonged protein–protein interactions in live cells. Cell Signal 18(10):1664–1670. doi:10.1016/j.cellsig.2006.01.004
47. Green AA, McElroy WD (1956) Crystalline firefly luciferase. Biochim Biophys Acta 20(1):170–176
48. Chiu NH, Christopoulos TK (1999) Two-site expression immunoassay using a firefly luciferase-coding DNA label. Clin Chem 45(11):1954–1959
49. Arai R, Nakagawa H, Kitayama A, Ueda H, Nagamune T (2002) Detection of protein–protein interaction by bioluminescence resonance energy transfer from firefly luciferase to red fluorescent protein. J Biosci Bioeng 94(4):362–364. doi:10.1263/jbb.94.362
50. Branchini BR, Rosenberg JC, Ablamsky DM, Taylor KP, Southworth TL, Linder SJ (2011) Sequential bioluminescence resonance energy transfer–fluorescence resonance energy transfer-based ratiometric protease assays with fusion proteins of firefly luciferase and red fluorescent protein. Anal Biochem 414(2):239–245. doi:10.1016/j.ab.2011.03.031
51. Yamakawa Y, Ueda H, Kitayama A, Nagamune T (2002) Rapid homogeneous immunoassay of peptides based on bioluminescence resonance energy transfer from firefly luciferase. J Biosci Bioeng 93(6):537–542. doi:10.1016/S1389-1723(02)80234-1
52. Branchini BR, Rosenberg JC, Ablamsky DM, Taylor KP, Southworth TL, Linder SJ (2011) Sequential bioluminescence resonance energy transfer-fluorescence resonance energy transfer-based ratiometric protease assays with fusion proteins of firefly luciferase and red fluorescent protein. Anal Biochem 414(2):239–245. doi:10.1016/j.ab.2011.03.031
53. Branchini BR, Ablamsky DM, Davis AL, Southworth TL, Butler B, Fan F, Jathoul AP, Pule MA (2010) Red-emitting luciferases for bioluminescence reporter and imaging applications. Anal Biochem 396(2):290–297. doi:10.1016/j.ab.2009.09.009
54. Naumov P, Ozawa Y, Ohkubo K, Fukuzumi S (2009) Structure and spectroscopy of oxyluciferin, the light emitter of the firefly bioluminescence. J Am Chem Soc 131(32):11590–11605. doi:10.1021/ja904309q
55. Takenaka Y, Masuda H, Yamaguchi A, Nishikawa S, Shigeri Y, Yoshida Y, Mizuno H (2008) Two forms of secreted and thermostable luciferases from the marine copepod crustacean. Metridia pacifica Gene 425(1–2):28–35. doi:10.1016/j.gene.2008.07.041
56. Markova SV, Burakova LP, Vysotski ES (2012) High-active truncated luciferase of copepod Metridia longa. Biochem Biophys Res Commun 417(1):98–103. doi:10.1016/j.bbrc.2011.11.063
57. Inouye S, Watanabe K, Nakamura H, Shimomura O (2000) Secretional luciferase of the luminous shrimp Oplophorus gracilirostris: cDNA cloning of a novel imidazopyrazinone luciferase(1). FEBS Lett 481(1):19–25
58. Gammon ST, Villalobos VM, Roshal M, Samrakandi M, Piwnica-Worms D (2009) Rational design of novel red-shifted BRET pairs: platforms for real-time single-chain protease biosensors. Biotechnol Prog 25(2):559–569. doi:10.1002/btpr.144
59. Li F, Yu J, Zhang Z, Cui Z, Wang D, Wei H, Zhang XE (2012) Buffer enhanced bioluminescence resonance energy transfer sensor based on Gaussia luciferase for in vitro detection of protease. Anal Chim Acta 724:104–110. doi:10.1016/j.aca.2012.02.047
60. Otsuji T, Okuda-Ashitaka E, Kojima S, Akiyama H, Ito S, Ohmiya Y (2004) Monitoring for dynamic biological processing by intramolecular bioluminescence resonance energy transfer system using secreted luciferase. Anal Biochem 329(2):230–237. doi:10.1016/j.ab.2004.03.010
61. Tannous BA, Kim DE, Fernandez JL, Weissleder R, Breakefield XO (2005) Codon-optimized Gaussia luciferase cDNA for mammalian gene expression in culture and in vivo. Mol Ther 11(3):435–443. doi:10.1016/j.ymthe.2004.10.016
62. Thompson EM, Nagata S, Tsuji FI (1989) Cloning and expression of cDNA for the luciferase from the marine ostracod Vargula hilgendorfii. Proc Natl Acad Sci USA 86(17):6567–6571

63. Shaner NC, Steinbach PA, Tsien RY (2005) A guide to choosing fluorescent proteins. Nat Methods 2(12):905–909. doi:10.1038/nmeth819
64. Prasher DC, Eckenrode VK, Ward WW, Prendergast FG, Cormier MJ (1992) Primary structure of the Aequorea victoria green-fluorescent protein. Gene 111(2):229–233
65. Wang Y, Shyy JY, Chien S (2008) Fluorescence proteins, live-cell imaging, and mechanobiology: seeing is believing. Annu Rev Biomed Eng 10:1–38. doi:10.1146/annurev.bioeng.010308.161731
66. Muller-Taubenberger A, Anderson KI (2007) Recent advances using green and red fluorescent protein variants. Appl Microbiol Biotechnol 77(1):1–12. doi:10.1007/s00253-007-1131-5
67. Griesbeck O, Baird GS, Campbell RE, Zacharias DA, Tsien RY (2001) Reducing the environmental sensitivity of yellow fluorescent protein. Mechanism and applications. J Biol Chem 276(31):29188–29194. doi:10.1074/jbc.M102815200
68. Nagai T, Ibata K, Park ES, Kubota M, Mikoshiba K, Miyawaki A (2002) A variant of yellow fluorescent protein with fast and efficient maturation for cell-biological applications. Nat Biotechnol 20(1):87–90. doi:10.1038/nbt0102-87
69. Nguyen AW, Daugherty PS (2005) Evolutionary optimization of fluorescent proteins for intracellular FRET. Nat Biotechnol 23(3):355–360. doi:10.1038/nbt1066
70. Matz MV, Fradkov AF, Labas YA, Savitsky AP, Zaraisky AG, Markelov ML, Lukyanov SA (1999) Fluorescent proteins from nonbioluminescent Anthozoa species. Nat Biotechnol 17(10):969–973. doi:10.1038/13657
71. Baird GS, Zacharias DA, Tsien RY (2000) Biochemistry, mutagenesis, and oligomerization of DsRed, a red fluorescent protein from coral. Proc Natl Acad Sci USA 97(22):11984–11989. doi:10.1073/pnas.97.22.11984
72. Campbell RE, Tour O, Palmer AE, Steinbach PA, Baird GS, Zacharias DA, Tsien RY (2002) A monomeric red fluorescent protein. Proc Natl Acad Sci USA 99(12):7877–7882. doi:10.1073/pnas.082243699
73. Bevis BJ, Glick BS (2002) Rapidly maturing variants of the Discosoma red fluorescent protein (DsRed). Nat Biotechnol 20(1):83–87. doi:10.1038/nbt0102-83
74. Shaner NC, Campbell RE, Steinbach PA, Giepmans BN, Palmer AE, Tsien RY (2004) Improved monomeric red, orange and yellow fluorescent proteins derived from Discosoma sp. red fluorescent protein. Nat Biotechnol 22(12):1567–1572. doi:10.1038/nbt1037
75. Wang L, Jackson WC, Steinbach PA, Tsien RY (2004) Evolution of new nonantibody proteins via iterative somatic hypermutation. Proc Natl Acad Sci USA 101(48):16745–16749. doi:10.1073/pnas.0407752101
76. Merzlyak EM, Goedhart J, Shcherbo D, Bulina ME, Shcheglov AS, Fradkov AF, Gaintzeva A, Lukyanov KA, Lukyanov S, Gadella TW, Chudakov DM (2007) Bright monomeric red fluorescent protein with an extended fluorescence lifetime. Nat Methods 4(7):555–557. doi:10.1038/nmeth1062
77. Shcherbo D, Merzlyak EM, Chepurnykh TV, Fradkov AF, Ermakova GV, Solovieva EA, Lukyanov KA, Bogdanova EA, Zaraisky AG, Lukyanov S, Chudakov DM (2007) Bright far-red fluorescent protein for whole-body imaging. Nat Methods 4(9):741–746. doi:10.1038/nmeth1083
78. Shcherbo D, Murphy CS, Ermakova GV, Solovieva EA, Chepurnykh TV, Shcheglov AS, Verkhusha VV, Pletnev VZ, Hazelwood KL, Roche PM, Lukyanov S, Zaraisky AG, Davidson MW, Chudakov DM (2009) Far-red fluorescent tags for protein imaging in living tissues. Biochem J 418(3):567–574. doi:10.1042/BJ20081949
79. Morozova KS, Piatkevich KD, Gould TJ, Zhang J, Bewersdorf J, Verkhusha VV (2010) Far-red fluorescent protein excitable with red lasers for flow cytometry and superresolution STED nanoscopy. Biophys J 99(2):L13–L15. doi:10.1016/j.bpj.2010.04.025
80. Tsien RY (1998) The green fluorescent protein. Annu Rev Biochem 67:509–544. doi:10.1146/annurev.biochem.67.1.509

81. Karasawa S, Araki T, Nagai T, Mizuno H, Miyawaki A (2004) Cyan-emitting and orange-emitting fluorescent proteins as a donor/acceptor pair for fluorescence resonance energy transfer. Biochem J 381(Pt 1):307–312. doi:10.1042/BJ20040321
82. Carriba P, Navarro G, Ciruela F, Ferre S, Casado V, Agnati L, Cortes A, Mallol J, Fuxe K, Canela EI, Lluis C, Franco R (2008) Detection of heteromerization of more than two proteins by sequential BRET-FRET. Nat Methods 5(8):727–733. doi:10.1038/nmeth.1229
83. Navarro G, Aymerich MS, Marcellino D, Cortes A, Casado V, Mallol J, Canela EI, Agnati L, Woods AS, Fuxe K, Lluis C, Lanciego JL, Ferre S, Franco R (2009) Interactions between calmodulin, adenosine A2A, and dopamine D2 receptors. J Biol Chem 284(41):28058–28068. doi:10.1074/jbc.M109.034231
84. Heroux M, Hogue M, Lemieux S, Bouvier M (2007) Functional calcitonin gene-related peptide receptors are formed by the asymmetric assembly of a calcitonin receptor-like receptor homo-oligomer and a monomer of receptor activity-modifying protein-1. J Biol Chem 282(43):31610–31620. doi:10.1074/jbc.M701790200
85. Navarro G, Carriba P, Gandia J, Ciruela F, Casado V, Cortes A, Mallol J, Canela EI, Lluis C, Franco R (2008) Detection of heteromers formed by cannabinoid CB1, dopamine D2, and adenosine A2A G-protein-coupled receptors by combining bimolecular fluorescence complementation and bioluminescence energy transfer. Sci World J 8:1088–1097. doi:10.1100/tsw.2008.136
86. Urizar E, Yano H, Kolster R, Gales C, Lambert N, Javitch JA (2011) CODA-RET reveals functional selectivity as a result of GPCR heteromerization. Nat Chem Biol 7(9):624–630. doi:10.1038/nchembio.623
87. Guo W, Urizar E, Kralikova M, Mobarec JC, Shi L, Filizola M, Javitch JA (2008) Dopamine D2 receptors form higher order oligomers at physiological expression levels. EMBO J 27(17):2293–2304. doi:10.1038/emboj.2008.153
88. Hu K, Clement JF, Abrahamyan L, Strebel K, Bouvier M, Kleiman L, Mouland AJ (2005) A human immunodeficiency virus type 1 protease biosensor assay using bioluminescence resonance energy transfer. J Virol Methods 128(1–2):93–103. doi:10.1016/j.jviromet.2005.04.012
89. Oka T, Takagi H, Tohya Y, Murakami K, Takeda N, Wakita T, Katayama K (2011) Bioluminescence technologies to detect calicivirus protease activity in cell-free system and in infected cells. Antiviral Res 90(1):9–16. doi:10.1016/j.antiviral.2011.02.002
90. Dacres H, Dumancic MM, Horne I, Trowell SC (2009) Direct comparison of bioluminescence-based resonance energy transfer methods for monitoring of proteolytic cleavage. Anal Biochem 385(2):194–202. doi:10.1016/j.ab.2008.10.040
91. Rogers KL, Picaud S, Roncali E, Boisgard R, Colasante C, Stinnakre J, Tavitian B, Brulet P (2007) Non-invasive in vivo imaging of calcium signaling in mice. PLoS ONE 2(10):e974. doi:10.1371/journal.pone.0000974
92. Baubet V, Le Mouellic H, Campbell AK, Lucas-Meunier E, Fossier P, Brulet P (2000) Chimeric green fluorescent protein-aequorin as bioluminescent $Ca^{2+}$ reporters at the single-cell level. Proc Natl Acad Sci USA 97(13):7260–7265. doi:10.1073/pnas.97.13.7260
93. Bakayan A, Vaquero CF, Picazo F, Llopis J (2011) Red fluorescent protein-aequorin fusions as improved bioluminescent Ca2+ reporters in single cells and mice. PLoS ONE 6(5):e19520. doi:10.1371/journal.pone.0019520
94. Miyawaki A, Llopis J, Heim R, McCaffery JM, Adams JA, Ikura M, Tsien RY (1997) Fluorescent indicators for Ca2+ based on green fluorescent proteins and calmodulin. Nature 388(6645):882–887. doi:10.1038/42264
95. Miyawaki A, Griesbeck O, Heim R, Tsien RY (1999) Dynamic and quantitative Ca2+ measurements using improved cameleons. Proc Natl Acad Sci USA 96(5):2135–2140
96. Romoser VA, Hinkle PM, Persechini A (1997) Detection in living cells of Ca2+ -dependent changes in the fluorescence emission of an indicator composed of two green fluorescent protein variants linked by a calmodulin-binding sequence. A new class of fluorescent indicators. J Biol Chem 272(20):13270–13274

97. Saito K, Hatsugai N, Horikawa K, Kobayashi K, Matsu-Ura T, Mikoshiba K, Nagai T (2010) Auto-luminescent genetically-encoded ratiometric indicator for real-time Ca2+ imaging at the single cell level. PLoS ONE 5(4):e9935. doi:10.1371/journal.pone.0009935
98. De A, Gambhir SS (2005) Noninvasive imaging of protein–protein interactions from live cells and living subjects using bioluminescence resonance energy transfer. FASEB J 19(14):2017–2019. doi:10.1096/fj.05-4628fje
99. Bjornsti MA, Houghton PJ (2004) The TOR pathway: a target for cancer therapy. Nat Rev Cancer 4(5):335–348. doi:10.1038/nrc1362
100. Kroeger KM, Hanyaloglu AC, Seeber RM, Miles LE, Eidne KA (2001) Constitutive and agonist-dependent homo-oligomerization of the thyrotropin-releasing hormone receptor. Detection in living cells using bioluminescence resonance energy transfer. J Biol Chem 276(16):12736–12743. doi:10.1074/jbc.M011311200
101. Mercier JF, Salahpour A, Angers S, Breit A, Bouvier M (2002) Quantitative assessment of beta 1- and beta 2-adrenergic receptor homo- and heterodimerization by bioluminescence resonance energy transfer. J Biol Chem 277(47):44925–44931. doi:10.1074/jbc.M205767200
102. Ayoub MA, Couturier C, Lucas-Meunier E, Angers S, Fossier P, Bouvier M, Jockers R (2002) Monitoring of ligand-independent dimerization and ligand-induced conformational changes of melatonin receptors in living cells by bioluminescence resonance energy transfer. J Biol Chem 277(24):21522–21528. doi:10.1074/jbc.M200729200
103. Pfleger KD, Eidne KA (2005) Monitoring the formation of dynamic G-protein-coupled receptor-protein complexes in living cells. Biochem J 385(Pt 3):625–637. doi:10.1042/BJ20041361
104. Boute N, Pernet K, Issad T (2001) Monitoring the activation state of the insulin receptor using bioluminescence resonance energy transfer. Mol Pharmacol 60(4):640–645
105. Issad T, Blanquart C, Gonzalez-Yanes C (2007) The use of bioluminescence resonance energy transfer for the study of therapeutic targets: application to tyrosine kinase receptors. Exp Opin Ther Targets 11(4):541–556. doi:10.1517/14728222.11.4.541
106. Tan PK, Wang J, Littler PL, Wong KK, Sweetnam TA, Keefe W, Nash NR, Reding EC, Piu F, Brann MR, Schiffer HH (2007) Monitoring interactions between receptor tyrosine kinases and their downstream effector proteins in living cells using bioluminescence resonance energy transfer. Mol Pharmacol 72(6):1440–1446. doi:10.1124/mol.107.039636
107. Sato M, Ozawa T, Inukai K, Asano T, Umezawa Y (2002) Fluorescent indicators for imaging protein phosphorylation in single living cells. Nat Biotechnol 20(3):287–294
108. Schroder M, Kroeger KM, Volk HD, Eidne KA, Grutz G (2004) Preassociation of nonactivated STAT3 molecules demonstrated in living cells using bioluminescence resonance energy transfer: a new model of STAT activation? J Leukoc Biol 75(5):792–797. doi:10.1189/jlb.1003496
109. Arai R, Nakagawa H, Tsumoto K, Mahoney W, Kumagai I, Ueda H, Nagamune T (2001) Demonstration of a homogeneous noncompetitive immunoassay based on bioluminescence resonance energy transfer. Anal Biochem 289(1):77–81. doi:10.1006/abio.2000.4924
110. Walls ZF, Gambhir SS (2008) BRET-based method for detection of specific RNA species. Bioconjug Chem 19(1):178–184. doi:10.1021/bc700278n
111. Andou T, Endoh T, Mie M, Kobatake E (2011) Development of an RNA detection system using bioluminescence resonance energy transfer. Sensor Actuat B Chem 152(2):277–284. doi:10.1016/j.snb.2010.12.020
112. So MK, Xu C, Loening AM, Gambhir SS, Rao J (2006) Self-illuminating quantum dot conjugates for in vivo imaging. Nat Biotechnol 24(3):339–343. doi:10.1038/nbt1188
113. Frasco MF, Chaniotakis N (2009) Semiconductor quantum dots in chemical sensors and biosensors. Sensors 9(9):7266–7286. doi:10.3390/s90907266
114. Xia Z, Xing Y, So MK, Koh AL, Sinclair R, Rao J (2008) Multiplex detection of protease activity with quantum dot nanosensors prepared by intein-mediated specific bioconjugation. Anal Chem 80(22):8649–8655. doi:10.1021/ac801562f

115. Kumar M, Zhang D, Broyles D, Deo SK (2011) A rapid, sensitive, and selective bioluminescence resonance energy transfer (BRET)-based nucleic acid sensing system. Biosens Bioelectron 30(1):133–139. doi:10.1016/j.bios.2011.08.043
116. Wu C, Mino K, Akimoto H, Kawabata M, Nakamura K, Ozaki M, Ohmiya Y (2009) In vivo far-red luminescence imaging of a biomarker based on BRET from Cypridina bioluminescence to an organic dye. Proc Natl Acad Sci USA 106(37):15599–15603. doi:10.1073/pnas.0908594106
117. Branchini BR, Ablamsky DM, Rosenberg JC (2010) Chemically modified firefly luciferase is an efficient source of near-infrared light. Bioconjug Chem 21(11):2023–2030. doi:10.1021/bc100256d
118. Yu J, Guan M, Li F, Zhang Z, Wang C, Shu C, Wei H, Zhang XE (2012) Effects of fullerene derivatives on bioluminescence and application for protease detection. Chem Commun 48(89):11011–11013. doi:10.1039/c2cc36099c
119. Xu X, Soutto M, Xie Q, Servick S, Subramanian C, von Arnim AG, Johnson CH (2007) Imaging protein interactions with bioluminescence resonance energy transfer (BRET) in plant and mammalian cells and tissues. Proc Natl Acad Sci USA 104(24):10264–10269. doi:10.1073/pnas.0701987104
120. Coulon V, Audet M, Homburger V, Bockaert J, Fagni L, Bouvier M, Perroy J (2008) Subcellular imaging of dynamic protein interactions by bioluminescence resonance energy transfer. Biophys J 94(3):1001–1009. doi:10.1529/biophysj.107.117275